

## Section 1

# Simultaneous Equation Solver

The simultaneous equation solver is a method for finding the solution  $\mathbf{u}$  of a linear matrix equation in the form shown in equation (5.1.1):

$$\mathbf{K}\mathbf{u} = \mathbf{p} \quad (5.1.1)$$

Simultaneous equation solvers are not only used for linear static structural analysis, but also for all types of analysis such as eigenvalue analysis, dynamic analysis, nonlinear analysis, etc. General solvers include the Gauss elimination method, direct solver based on the decomposition method, and the iterative solver, which converges to a solution that minimizes iterative calculations. Direct solver is generally used for structural analysis because it is not affected by the numerical properties of matrices and can find the solution safely. However, when the size of the problem increases, the memory capacity and computation amount tend to increase rapidly. Hence, the iterative solver is recommended for large problems because it requires relatively less memory capacity. However for structural analysis, the iterative solver may not provide the wanted solution due to the numerical properties of matrices, and the number of iterative calculations needed to obtain the converging solution may be large. GTS NX provides a function that automatically determines the direct solver or iterative solver, depending on the size of the problem in question.

In direct solver, the simultaneous equation solution is found in two steps. The first step is matrix decomposition and the second step is the forward-backward substitution (FBS) process. The  $LU$  solver, generally used for asymmetric matrices, can be applied to matrix decomposition in the following form for the symmetric stiffness matrix  $\mathbf{K}$  obtained in finite element analysis.

$$\mathbf{L}\mathbf{L}^T\mathbf{u} = \mathbf{p} \text{ or } \mathbf{L}\mathbf{D}\mathbf{L}^T\mathbf{u} = \mathbf{p} \quad (5.1.2)$$

$\mathbf{L}$  : Lower triangular matrix

$\mathbf{D}$  : Diagonal matrix

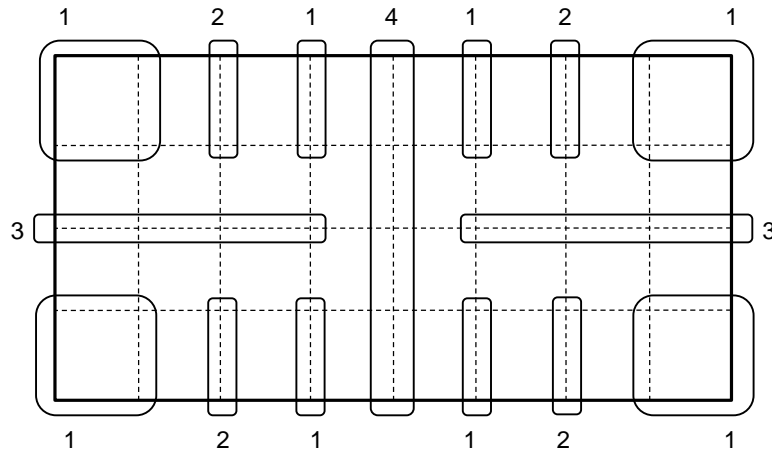
Generally, the matrix decomposition method that includes  $\mathbf{D}$  is needed when the stiffness matrix is not definitely positive. GTS NX uses the  $\mathbf{L}\mathbf{L}^T$  form matrix decomposition method (Cholesky decomposition method) for linear static structural analysis. For eigenvalue analysis or nonlinear analysis, the positive definite condition cannot be guaranteed and so, the  $\mathbf{L}\mathbf{D}\mathbf{L}^T$  form matrix decomposition method is used.

When applying the direct solver, the sparse matrix needs to be applied appropriately. Generally, the stiffness matrix  $\mathbf{K}$  generated in finite element analysis is a sparse matrix with multiple '0', and the

required memory capacity and computation amount differs greatly depending on how this sparsity is used. Hence, GTS NX not only provides the direct solver for general dense matrices that do not use the sparse matrix, but also provides the multi-frontal solver, which appropriately uses the sparse matrix to greatly reduce the memory capacity and computation amount.

The multi-frontal solver requires reordering of DOFs to minimize the memory capacity and computation amount using the sparse matrix, and matrix decomposition is performed by separating the matrix into multiple fronts according to this reordered information. Figure 5.1.1 displays the effective computation order of a rectangular mesh generated by DOF reordering. The algorithm used to implement DOF reordering is a recursive bisection, and forward substitution is done in the same order as the matrix decomposition whilst backward substitution is done in the opposite order.

Figure 5.1.1 Matrix decomposition order of multi-frontal solver



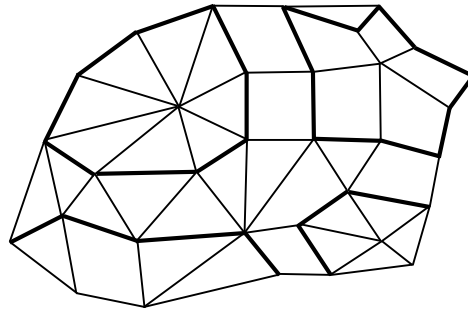
The multi-frontal solver used in GTS NX does not assemble and save the stiffness matrix of the entire region individually and hence, requires less memory capacity than the general multi-frontal solver. The out-of-core analysis function is supported to provide additional hard disk memory automatically during memory shortage when solving large problems.

Also, implementation of the multi-frontal solver uses the computation ability of the Graphics Processing Unit (GPU) to process calculations. The recent demand for complex problems highlights the importance of the simultaneous equation solver performance, which is the core of finite element analysis. The GPU consists of multiple computation units (cores) and provide a much higher computational performance than the CPU. The GPU is applied to real matrix decomposition, which takes the longest computation time, to provide an overall improved computational performance.

The iterative solver is a method of reducing the error of the approximate solution through iterative calculations and so, it is very important to reduce the convergence error using only a small number of calculations. Generally, the number of iterative calculations is determined by the preconditioning

method. GTS NX uses the SA(smoothed aggregation) AMG(algebraic multi-grid)<sup>1</sup> methods which are preconditioning methods that are known to be stable, regardless of the element shape. The number of calculations of the AMG method is not greatly affected by the number of DOF because it uses a multi-grid, and this method displays stable convergence when used on elements that have displacement and rotation nodal DOFs such as shell elements. The multi-grid is composed automatically for the iterative solver using the AMG method, and this is created by the representative DOFs of the adjacent node set and each node set.

Figure 5.1.2 Example of node set for multi-grid composition



As explained above, the performance of the direct solver and iterative solver differ on the size of the problem and GTS NX provides an automatic selection function to determine the solver. When using the automatic section function, the direct solver using the dense matrix is selected for small size problems, the multi-frontal solver is selected for medium size problems and the AMG iterative solver is selected for large size problems.

The automatic selection criterion is determined by considering the following points.

- ▶ When empirical condition is known : Determined with reference to the number of user input nodes or elements
- ▶ When empirical condition is unknown : Determined within the program with reference to the number of model DOF and system memory size

## Section 2 Eigenvalue Extraction

Eigenvalue extraction is a fundamental algorithm of normal mode analysis, and the eigenvalue extraction problems in normal mode analysis have the following form.

$$\mathbf{K}\phi - \lambda_r \mathbf{B}\phi = \mathbf{0} \quad (\text{no summation}) \quad (5.2.1)$$

**K** : Stiffness matrix

**B** : Mass matrix (**M**) when performing normal mode analysis

The eigenvalue extraction method in GTS NX is coupled and changes with the simultaneous equation solver. The Lanczos resampling is used for the multi-frontal solver (the default value of the simultaneous equation solver), and eigenvalue extraction or direct solver using the dense matrix is used for the dense matrix solver. Each method has the following characteristics.

- Lanczos resampling
  - ▶ Appropriate for large sized problems.
  - ▶ Because the eigenvalue can be omitted, use of the Sturm sequence check option is recommended.
- Direct solver using the dense matrix
  - ▶ The performance can suddenly decrease when the number of DOF is around  $10^3$  and so, it is appropriate for small scale test models.
  - ▶ The eigenvalue is not omitted.

Lanczos resampling is a method of finding the approximate eigenvalue using the tridiagonal matrix that arises when generating the Krylov subspace  $\text{span}(\mathbf{v}_1, \mathbf{v}_2, \dots, \mathbf{v}_k)$ <sup>1</sup>. For effective eigenvalue calculation, the block tridiagonal matrix<sup>2</sup> can be used, and because the tridiagonal matrix size is maintained similar to the number of eigenvalues, the computation speed is very fast and it is appropriate for large scale problems. However, eigenvalue omission can occur and so, it is useful to use the checking option.

The direct solver using the dense matrix goes through the stiffness matrix decomposition, tridiagonal matrix generation and eigenvalue calculation processes. Tridiagonal matrix generation and eigenvalue calculation is done for the entire matrix and eigenvalue omission does not occur. However, it is inappropriate for solving large size problems.

<sup>1</sup> Hughes, T.J.R., The Finite Element Method, Prentice-Hall International, Inc., New Jersey, 1987

<sup>2</sup> Cullum, J. and Donath, W., "A Block Lanczos algorithms for computing the q algebraically largest eigenvalues and a corresponding eigenspace of large real symmetric matrices," Proc. 1974 IEEE Conference on Decision and Control, IEEE Computer Society, 1974

**Eigenvalue computation range**

For normal mode analysis, the number of eigenvalues and its range considers the modal participation factor (equation 5.3.1) or modal effective mass (equation 5.3.3), or can be determined with reference to the frequency region of interest. If the number and range of eigenvalues is determined, it can be set using the following inputs.

Table 5.2.1 Setting the number and range of eigenvalues

Variable setting ( $v_1$ , $v_2$ , $N$ input or not input)	Eigenvalue range	Number of eigenvalues
$v_1$ , $v_2$ , $N$	$v_1 < v < v_2$	Maximum $N$
$v_1$ , <b>not input</b> , $N$	$v_1 < v$	Maximum $N$
<b>not input</b> , $v_2$ , $N$	$v < v_2$	Maximum $N$
<b>not input</b> , <b>not input</b> , $N$	$-\infty < v < \infty$	Maximum $N$
$v_1$ , $v_2$ , <b>not input</b>	$v_1 < v < v_2$	All eigenvalues
$v_1$ , <b>not input</b> , <b>not input</b>	$v_1 < v$	All eigenvalues
<b>not input</b> , $v_2$ , <b>not input</b>	$v < v_2$	All eigenvalues
<b>not input</b> , <b>not input</b> , <b>not input</b>	$-\infty < v < \infty$	All eigenvalues

The  $v_1$ ,  $v_2$  inputs above are the frequency (Hz) in normal mode analysis.

**Eigenvalue computation results**

Eigenvectors, which are the results of the eigenvalue problem, satisfy equation (5.2.2), even if its size changes.

$$\begin{aligned} a(\mathbf{K}\phi_i - \lambda_i\mathbf{B}\phi_i) &= \mathbf{K}\varphi_i - \lambda_i\mathbf{B}\varphi_i = \mathbf{0} \\ \varphi_i &= a\phi_i \end{aligned} \quad (5.2.2)$$

Hence, a method is needed to express the size of the calculated eigenvalue consistently. GTS NX applies the eigenvector normalization process such that the following equation is satisfied, depending on the analysis type.

$$\phi_i^T \mathbf{M} \phi_i = 1 \quad (5.2.3)$$

The eigenvalue calculation algorithm is only an approximate solution, even when the direct solver for the dense matrix is used, and its accuracy cannot be guaranteed. Therefore, GTS NX selects the following values as the eigenvalue calculation results to check the accuracy of the calculated eigenvalue and eigenvector.



Table 5.2.2 Calculation results excluding eigenvalue and eigenvector

Result article	Calculation
<b>Generalized mass</b>	$b_i = \phi_i^T \mathbf{B} \phi_i$
<b>Generalized stiffness</b>	$k_i = \phi_i^T \mathbf{K} \phi_i$
<b>Orthogonality loss</b>	$\delta_i = \max\left(\frac{\phi_{i-1}^T \mathbf{K} \phi_i}{k_i}, \frac{\phi_{i-1}^T \mathbf{B} \phi_i}{b_i}\right)$
<b>Error measure</b>	$e_i = \frac{\ \mathbf{K} \phi_i - \lambda_i \mathbf{B} \phi_i\ }{\ \mathbf{K} \phi_i\ }$

## Section 3

# Effective Mass and Mode Superposition

## 3.1

## Effective Mass

After calculating the natural frequency, natural period and mode shape using mode analysis, these can be used to compute useful information such as modal effective mass or modal participation factor. The  $i$ th modal participation factor is expressed as  $\Gamma_{i\alpha}$  and can be calculated as follows:

$$\Gamma_{i\alpha} = \frac{1}{m_i} \phi_i^T \mathbf{M} \mathbf{T}_\alpha, \quad \alpha = 1, 2, 3, 4, 5, 6 \quad (\text{no summation}) \quad (5.3.1)$$

$$m_i = \phi_i^T \mathbf{M} \phi_i \quad (\text{generalized mass})$$

$\alpha$  : DOF direction (1~3 : displacement, 4~6 : rotation)

Here,  $\mathbf{T}_\alpha$  is the matrix that represents the size of the directional stiffness behavior and it is defined for each node to have the following property:

$$\begin{bmatrix} 1 & 0 & 0 & 0 & z - z_0 & y_0 - y \\ 0 & 1 & 0 & z_0 - z & 0 & x - x_0 \\ 0 & 0 & 1 & y - y_0 & x_0 - x & 0 \\ 0 & 0 & 0 & 1 & 0 & 0 \\ 0 & 0 & 0 & 0 & 1 & 0 \\ 0 & 0 & 0 & 0 & 0 & 1 \end{bmatrix} \begin{Bmatrix} e_1 \\ e_2 \\ e_3 \\ e_4 \\ e_5 \\ e_6 \end{Bmatrix}, \quad e_\beta = \delta_{\alpha\beta} \quad (5.3.2)$$

$x_0, y_0, z_0$  represent the center of rotation. GTS NX sets it as an arbitrary node or the center of mass for the entire model.

The modal effective mass is also defined for each direction and can be simply calculated using the modal participation factor as follows:

$$m_{i\alpha}^{\text{eff}} = (\Gamma_{i\alpha})^2 m_i \quad (5.3.3)$$

Adding the effective mass for all modes is the same as the mass of the entire model, excluding the nodes that have assigned constraint conditions.

## 3.2

### Mode Superposition

The mode superposition method can be applied to dynamic response analysis. Mode superposition uses the eigenmode found from eigenvalue analysis (instead of directly solving the linear dynamic equilibrium equation) to solve the size reduced mode equilibrium equation as shown below:

$$\mathbf{M}\ddot{\mathbf{u}}(t) + \mathbf{C}\dot{\mathbf{u}}(t) + \mathbf{K}\mathbf{u}(t) = \mathbf{f}(t) \quad (5.3.4)$$

The spatial coordinate system displacement  $\mathbf{u}(t)$  can be expressed as a combination of the modal displacement  $\xi(t)$  using the eigenmode shape  $\Phi$  as follows:

$$\mathbf{u}(t) = \Phi \xi(t), \quad \Phi = [\phi_1 \quad \phi_2 \quad \dots \quad \phi_N] \quad (5.3.5)$$

Using this, the dynamic equilibrium equation (5.3.4) can be expressed in the modal coordinate system as follows:

$$[\Phi^T \mathbf{M} \Phi] \ddot{\xi}(t) + [\Phi^T \mathbf{C} \Phi] \dot{\xi}(t) + [\Phi^T \mathbf{K} \Phi] \xi(t) = \Phi^T \mathbf{f}(t) \quad (5.3.6)$$

Generally when mode superposition is applied, the high order modes are excluded and only partial low order modes are used to compose the eigenmode shape  $\Phi$  and so, equation (5.3.6) is an approximation of equation (5.3.4). Hence, if an insufficient number of eigenmodes is included in the calculation for expressing the actual physical displacement, the accuracy of the calculated results can fall greatly.

The mode equilibrium equation (5.3.7) is expressed independently for each mode when the modal damping matrix  $\Phi^T \mathbf{C} \Phi$  is '0', as shown below:

$$m_i \ddot{\xi}_i(t) + k_i \xi_i(t) = p_i(t) \quad (5.3.7)$$

$m_i$  : i th modal mass                       $p_i$  : i th modal load  
 $k_i$  : i th modal stiffness                 $\xi_i$  : i th modal displacement

Using the mode superposition method above, the equilibrium equation can be reduced to have the same number of variables as the number of calculated eigenmodes, and analysis can be performed effectively when the mode equilibrium equation is fully separated between modes.

#### Damping term treatment

If the modal damping matrix is diagonalized and the coupling removed for the modal equilibrium equation (5.3.7) that is reduced using the eigenmode, it can be expressed as a separated form for each mode like equation (5.3.8).

$$m_i \ddot{\xi}_i(t) + b_i \dot{\xi}_i(t) + k_i \xi_i(t) = p_i(t) \quad (5.3.8)$$

$b_i$  :  $i$  th modal damping

Or, it can be expressed as follows.

$$\ddot{\xi}_i(t) + 2\zeta_i\omega_i\dot{\xi}_i(t) + \omega_i^2\xi_i(t) = \frac{1}{m_i} p_i(t) \quad (5.3.9)$$

$\zeta_i = b_i/(2m_i\omega_i)$  : Modal damping ratio

$\omega_i^2 = k_i/m_i$  : Modal frequency

The modal damping value can be input differently according to the frequency and in this case, the modal damping value is added to the modal damping matrix  $\Phi^T \mathbf{C} \Phi$ , which is composed of other general damping values such as mass-proportional damping, stiffness-proportional damping etc. Hence, modal separation of the modal equilibrium equation is possible when the modal damping matrix  $\Phi^T \mathbf{C} \Phi$  is a diagonal matrix, and this is applicable when the proportional damping coefficient and structural damping is constant for each element and when damping elements (spring, damper) do not exist. If not, the coupling between equilibrium equations of each mode, due to the un-diagonalized modal damping term, needs to be considered.

#### Enforced motion

When enforced motion is given in the mode superposition method, it cannot be applied directly to the modal equilibrium equation. GTS NX uses the following processes to apply enforced motion. Firstly, the equilibrium equation (5.3.4) is separated into the DOFs with and without enforced motion.

$$\begin{bmatrix} \mathbf{M}_{11} & \mathbf{M}_{12} \\ \mathbf{M}_{21} & \mathbf{M}_{22} \end{bmatrix} \begin{Bmatrix} \dot{\mathbf{u}}_1 \\ \dot{\mathbf{u}}_2 \end{Bmatrix} + \begin{bmatrix} \mathbf{C}_{11} & \mathbf{C}_{12} \\ \mathbf{C}_{21} & \mathbf{C}_{22} \end{bmatrix} \begin{Bmatrix} \dot{\mathbf{u}}_1 \\ \dot{\mathbf{u}}_2 \end{Bmatrix} + \begin{bmatrix} \mathbf{K}_{11} & \mathbf{K}_{12} \\ \mathbf{K}_{21} & \mathbf{K}_{22} \end{bmatrix} \begin{Bmatrix} \mathbf{u}_1 \\ \mathbf{u}_2 \end{Bmatrix} = \begin{Bmatrix} \mathbf{f}_1 \\ \mathbf{f}_2 \end{Bmatrix} \quad (5.3.10)$$

$\mathbf{u}_1$  : Displacement of unconfined DOF

$\mathbf{u}_2$  : Displacement of DOF confined by enforced motion

$\mathbf{f}_1$  : Load acting on unconfined DOF

$\mathbf{f}_2$  : Confining force of DOF confined by enforced motion

Separating the unconfined DOF displacement  $\mathbf{u}_1$  into the following quasi-static displacement  $\mathbf{u}_1^{qs}$  and dynamic relative displacement  $\mathbf{y}$  is as follows:

$$\begin{aligned} \mathbf{u}_1 &= \mathbf{u}_1^{qs} + \mathbf{y} \\ \mathbf{u}_1^{qs} &= -\mathbf{K}_{11}^{-1} \mathbf{K}_{12} \mathbf{u}_2 \end{aligned} \quad (5.3.11)$$

Rearranging for the dynamic relative displacement  $\mathbf{y}$ ,

$$\mathbf{M}_{11}\ddot{\mathbf{y}} + \mathbf{C}_{11}\dot{\mathbf{y}} + \mathbf{K}_{11}\mathbf{y} = \mathbf{f}_1 + (\mathbf{M}_{11}\mathbf{K}_{11}^{-1}\mathbf{K}_{12} - \mathbf{M}_{12})\ddot{\mathbf{u}}_2 \quad (5.3.12)$$

The damping related terms on the right hand side of the equation were ignored. Applying the mode superposition method and expressing the equation using the modal relative displacement  $\mathbf{y}(t) = \Phi_{11}\mathbf{x}(t)$  is as follows:

$$\begin{aligned} [\Phi_{11}^T \mathbf{M}_{11} \Phi_{11}] \ddot{\mathbf{x}} + [\Phi_{11}^T \mathbf{C}_{11} \Phi_{11}] \dot{\mathbf{x}} + [\Phi_{11}^T \mathbf{K}_{11} \Phi_{11}] \mathbf{x} &= \Phi_{11}^T [\mathbf{f}_1 + (\mathbf{M}_{11}\mathbf{K}_{11}^{-1}\mathbf{K}_{12} - \mathbf{M}_{12})\ddot{\mathbf{u}}_2] \\ \mathbf{u}_1 &= \mathbf{u}_1^{gs} + \mathbf{y} = -\mathbf{K}_{11}^{-1}\mathbf{K}_{12}\mathbf{u}_2 + \Phi_{11}\mathbf{x} \end{aligned} \quad (5.3.13)$$

If the  $\mathbf{K}_{11}$  has singularity because of an existing rigid-body mode in the structure, the singularity can be removed by appropriate shifting using the stiffness matrix  $\mathbf{K}_{11}$  and mass matrix  $\mathbf{M}_{11}$ .

#### Residual vector

As explained above, errors can occur due to high order modes that are not included in the eigenmode shape  $\Phi$  when using mode superposition. To reduce such errors, GTS NX uses the residual vector  $\mathbf{R}$ , which is composed perpendicular to the existing eigenmode, for the mass matrix  $\mathbf{M}$  and stiffness matrix  $\mathbf{K}$ .

$$\mathbf{R} = \mathbf{K}^{-1}(\mathbf{I} - \mathbf{M}\Phi\Phi^T)\mathbf{F} \quad (5.3.14)$$

Here,  $\mathbf{F}$  is generally composed of the load vector and the damping force is included when a damping element exists.

GTS NX uses the method suggested by Dickens<sup>3</sup> etc. to find the augmented mode shapes perpendicular to the residual vector  $\mathbf{R}$ . This is added to the existing eigenmode shape  $\Phi$  for applying mode superposition.

<sup>3</sup> J.M. Dickens, J.M. Nakagawa, and M.J. Wittbrodt, "A Critique of Mode Acceleration and Modal Truncation Augmentation Methods for Modal Response Analysis" Computers & Structures, Vol 62, No. 6, 1997, pp. 985-998

## Section 4 Dynamic Response

### 4.1 Time Integration

GTS NX uses direct time integration and mode superposition to obtain the transient response of the linear equation of motion shown in equation (5.3.4). For the direct time integration of linear problems, the implicit method is used.

#### Implicit direct integration

GTS NX uses the  $\alpha$  method (HHT- $\alpha$ )<sup>4</sup> suggested by Hilber, Hughes, Taylor for implicit direct integration. The HHT- $\alpha$  method is a general form of the Newmark method<sup>5</sup> and has a controllable numerical damping effect. Using this, the high frequency noise can be controlled and it has a 2 order accuracy for time steps, just like the Newmark method. The HHT- $\alpha$  method uses the following modified dynamic equilibrium equation:

$$\mathbf{M}\mathbf{a}^{n+1} + (1 + \alpha_H) [\mathbf{C}\mathbf{v}^{n+1} + \mathbf{f}^{\text{int},n+1} - \mathbf{f}^{\text{ext},n+1}] - \alpha_H [\mathbf{C}\mathbf{v}^n + \mathbf{f}^{\text{int},n} - \mathbf{f}^{\text{ext},n}] = \mathbf{0} \quad (5.4.1)$$

Here,  $\mathbf{a}^{n+1}$  and  $\mathbf{v}^{n+1}$  each represent the acceleration and velocity vector of the  $n+1$  th time step and  $\alpha_H \in [-1/3, 0]$  is the coefficient that determines the numerical damping effect. When considering the effects of non-mechanical strain, such as thermal expansion of the material, and the internal forces due to in-situ stress and pore pressure, the internal forces of linear analysis can be expressed as the following equation including the product of stiffness matrix and DOF.

$$\mathbf{f}^{\text{int},n+1} = \mathbf{K}\mathbf{u}^{n+1} - \mathbf{f}^{\text{nonmech},n+1} + \mathbf{f}^{\text{int},0} \quad (5.4.2)$$

Introducing the time step equation from the Newmark method, the velocity, displacement and acceleration at time steps  $n, n+1$  can be expressed using the following relationship:

$$\begin{aligned} \mathbf{v}^{n+1} &= \mathbf{v}^n + \Delta t [\gamma \mathbf{a}^{n+1} + (1 - \gamma) \mathbf{a}^n] \\ \mathbf{u}^{n+1} &= \mathbf{u}^n + \Delta t \mathbf{v}^n + \frac{1}{2} \Delta t^2 [2\beta \mathbf{a}^{n+1} + (1 - 2\beta) \mathbf{a}^n] \end{aligned} \quad (5.4.3)$$

Recomposing the equilibrium equation (5.4.1) using equations (5.4.2) and (5.4.3), the following simultaneous equation with the displacement at time  $n+1$  as a variable can be obtained as follows:

<sup>4</sup> H.M Hilber, T.J.R. Hughes, and R.L. Taylor, "Improved Numerical Dissipation for Time Integration Algorithms in Structural Dynamics," Earthquake Engineering and Structural Dynamics, Vol 5, No. 3, 1977, pp. 283-292

<sup>5</sup> M. Newmark, "A Method of Computation for Structural Dynamics," ASCE Journal of the Engineering Mechanics Division, Vol. 5, No. EM3, 1959, pp. 67-94

$$\begin{aligned}
\mathbf{K}^{eff} \mathbf{u}_{n+1} &= \mathbf{f}^{eff} \\
\mathbf{K}^{eff} &= \frac{1}{\beta \Delta t^2} \mathbf{M} + \frac{(1 + \alpha_H) \gamma}{\beta \Delta t} \mathbf{C} + (1 + \alpha_H) \mathbf{K}, \\
\mathbf{f}^{eff} &= -\mathbf{f}^{int,0} + (1 + \alpha_H) [\mathbf{f}^{ext,n+1} + \mathbf{f}^{nonmech,n+1}] - \alpha_H [\mathbf{f}^{ext,n} + \mathbf{f}^{nonmech,n}] + \\
&\mathbf{M} \left[ \frac{1}{\beta \Delta t^2} \mathbf{u}^n + \frac{1}{\beta \Delta t} \mathbf{v}^n + \left( \frac{1}{2\beta} - 1 \right) \mathbf{a}^n \right] + \\
&\mathbf{C} \left[ \frac{(1 + \alpha_H) \gamma}{\beta \Delta t} \mathbf{u}^n + \left\{ \frac{(1 + \alpha_H) \gamma}{\beta} - 1 \right\} \mathbf{v}^n + \Delta t (1 + \alpha_H) \left( \frac{\gamma}{2\beta} - 1 \right) \mathbf{a}^n \right] + \alpha_H \mathbf{K} \mathbf{u}^n
\end{aligned} \tag{5.4.4}$$

The right hand side  $\mathbf{f}^{eff}$  from equation (5.4.4) is determined by the internal force and calculated displacement, velocity, acceleration at time step  $n$ . When the right hand side is determined, the displacement vector  $\mathbf{u}_{n+1}$  at  $n+1$  can be calculated using the simultaneous equation solver explained in the section above. The velocity and acceleration at  $n+1$  can be obtained by substituting this calculated displacement into the Newmark time step equation (5.4.3). The transient response of the structure can be calculated by the time integration that repeats the processes outlined above.

The effective stiffness matrix ( $\mathbf{K}^{eff}$ ) in the left hand side of equation (5.4.4) reuses the once decomposed matrix when the time step is kept constant, allowing effective analysis by only repeating the front-back substitution process.

HHT- $\alpha$  time integration has unconditional stability when  $\gamma = (1 - 2\alpha_H) / 2$ ,  $\beta = (1 - \alpha_H)^2 / 4$  and when  $\alpha_H = 0$ . It is specialized in to the Newmark method that uses the average acceleration. GTS NX uses a default value of  $\alpha_H = -0.05$ .

#### Damping effect

GTS NX considers two types of damping: mass-proportional damping and stiffness-proportional damping. There is also mode damping, which is only applied for mode superposition as mentioned in section 5.3.2. The damping effects in linear time history analysis are applied to the damping matrix  $\mathbf{C}$  in the following form:

$$\mathbf{C} = \alpha_j^e \mathbf{M}_j^e + \beta_j^e \mathbf{K}_j^e + \mathbf{B} \tag{5.4.5}$$

$\alpha_j^e$  : Mass proportional damping coefficient for  $j$  th element

$\beta_j^e$  : Stiffness proportional damping coefficient for  $j$  th element

$\mathbf{M}_j^e$  : Mass matrix of  $j$ th element

$\mathbf{K}_j^e$  : Stiffness matrix of  $j$ th element

$\mathbf{B}$  : Damping matrix due to damping element (damper)

**Application of mode superposition**

To use time integration using mode superposition, the mass in the mode equilibrium equation (5.3.6) is set to '1' and rewritten as follows:

$$\begin{aligned} \ddot{\xi}_i(t) + \bar{C}_{ij}\dot{\xi}_j(t) + \omega_i^2\xi_i(t) &= p_i(t) = p_i(t - \Delta t) + \frac{\Delta p_i}{\Delta t}t \\ \bar{C}_{ij} &= [\bar{\mathbf{C}}]_{ij} = [\mathbf{\Phi}^T \mathbf{C} \mathbf{\Phi}]_{ij} \end{aligned} \quad (5.4.6)$$

Time integration using mode superposition can be classified into two types, depending on the ductile state of the mode damping matrix  $\bar{C}_{ij}$ :

**► Uncoupled system**

If the mode damping matrix  $\bar{C}_{ij}$  is diagonalized and the ductility is removed, the response is analyzed independently for each mode and the displacement and velocity of each time step is determined from the displacement and velocity of the previous time step using the following equation. The modal integral coefficients  $a_{\alpha\beta}^i, b_{\alpha\beta}^i$  at the  $i$  th mode can be obtained by finding the particular solution and homogeneous solution of (5.4.6) and applying it to the initial condition (displacement and velocity of the previous time step).

$$\begin{bmatrix} \xi_i^{n+1} \\ \dot{\xi}_i^{n+1} \end{bmatrix} = \begin{bmatrix} a_{11}^i & a_{12}^i \\ a_{21}^i & a_{22}^i \end{bmatrix} \begin{bmatrix} \xi_i^n \\ \dot{\xi}_i^n \end{bmatrix} + \begin{bmatrix} b_{11}^i & b_{12}^i \\ b_{21}^i & b_{22}^i \end{bmatrix} \begin{bmatrix} P_i^n \\ P_i^{n+1} \end{bmatrix} \quad (5.4.7)$$

**► Coupled system**

If ductility is not removed from the mode damping matrix, the ductility between modes needs to be considered and modal analysis cannot be performed independently. In this case, GTS NX separates the mode damping matrix into the following diagonal component ( $\bar{C}_{diag}$ ) and off-diagonal component ( $\bar{C}_{off}$ ) and treats the damping force of the off-diagonal component as an external force for analysis.

$$\bar{\mathbf{C}} = \bar{\mathbf{C}}_{diag} + \bar{\mathbf{C}}_{off} \quad (5.4.8)$$

In this case, all displacements are independent and the mode velocity is softened to compose the following simultaneous equation. If the time step is fixed, it can be solved without extra matrix decomposition, just like direct time integration.

$$\begin{bmatrix} \mathbf{I} & \mathbf{B}_{12} \bar{\mathbf{C}}_{off}^T \\ 0 & \mathbf{I} + \mathbf{B}_{22} \bar{\mathbf{C}}_{off}^T \end{bmatrix} \begin{bmatrix} \xi^{n+1} \\ \dot{\xi}^{n+1} \end{bmatrix} = \begin{bmatrix} \mathbf{A}_{11} & \mathbf{A}_{12} \\ \mathbf{A}_{21} & \mathbf{A}_{22} \end{bmatrix} \begin{bmatrix} \xi^n \\ \dot{\xi}^n \end{bmatrix} + \begin{bmatrix} \mathbf{B}_{11} & \mathbf{B}_{12} \\ \mathbf{B}_{21} & \mathbf{B}_{22} \end{bmatrix} \begin{bmatrix} \mathbf{p}^n - \bar{\mathbf{C}}_{off}^T \dot{\xi}^n \\ \mathbf{p}^{n+1} \end{bmatrix} \quad (5.4.9)$$

$$\mathbf{A}_{\alpha\beta} = \text{diag}(a_{\alpha\beta}^i), \quad \mathbf{B}_{\alpha\beta} = \text{diag}(b_{\alpha\beta}^i)$$

**Initial condition of mode superposition**

When initial displacement and initial velocity are given, the initial displacement  $\xi_i^0$  and initial velocity  $\dot{\xi}_i^0$  in the modal coordinate system is defined as follows. Using all modes gives an equation, and using partial modes gives an approximate relationship.

$$\begin{aligned}\xi_i^0 &= \frac{1}{m_i} \phi_i^T \mathbf{M} \mathbf{u}_0 \\ \dot{\xi}_i^0 &= \frac{1}{m_i} \phi_i^T \mathbf{M} \mathbf{v}_0\end{aligned}\quad (5.4.10)$$

$\phi_i$  :  $i$  th eigenmode shape

$\mathbf{u}_0$  : Initial displacement

$\mathbf{v}_0$  : Initial velocity

## 4.2

### Frequency Response

Frequency response analysis calculates the structural response under a load vibrating at a uniform frequency. All loads in frequency response analysis are defined in the frequency domain and expressed as a function of excitation frequency. In other words, the load in frequency response analysis can be expressed using the following complex harmonic function when the angular excitation frequency is  $\omega$ .

$$\mathbf{f}(t) = \mathbf{f}(\omega) e^{i\omega t} \quad (5.4.11)$$

The response can also be expressed in the same form.

$$\mathbf{u}(t) = \mathbf{u}(\omega) e^{i\omega t} \quad (5.4.12)$$

Using this, the equation of motion is expressed in the following form:

$$\left[ -\omega^2 \mathbf{M} + i\omega \mathbf{C} + \mathbf{K} \right] \mathbf{u}(\omega) = \mathbf{f}(\omega) \quad (5.4.13)$$

Here, both the load and displacement are expressed as complex numbers. When expressing the complex value using magnitude/phase angle, the magnitude represents the maximum load or displacement within the vibration period and the phase angle is the position (angle) at which this maximum value occurs. On the other hand, when expressing the complex value using real component/imaginary component, the real component is the load or displacement magnitude at the starting point of the vibration period and the imaginary component is the load or displacement after 1/4 period ( $\pi / 2$ ). Hence, the imaginary component changes with the vibration period. The relationship between magnitude/phase angle and real component/imaginary component is as follows:

$$\begin{aligned}
 u &= \sqrt{u_r^2 + u_i^2} && : \text{Magnitude} \\
 \theta &= \tan^{-1}(u_i / u_r) && : \text{Phase angle} \\
 u_r &= u \cos \theta && : \text{Real component} \\
 u_i &= u \sin \theta && : \text{Imaginary component}
 \end{aligned}$$

#### Direct frequency response analysis

When using the direct solver for direct frequency response analysis, solving the simultaneous equation (5.4.13) gives the frequency response  $\mathbf{u}(\omega)$ . If there is no damping, equation (5.4.13) is a real number simultaneous equation. But if there is damping, it is a complex number simultaneous equation. The solution can be found accurately using the direct method, but calculation is very inefficient for large problems or when many frequencies exist because the simultaneous equation needs to be recomposed and solved for each frequency.

## 4.3

### Response Spectrum

Response spectrum analysis is a method of evaluating the structural response due to base motion (uniform shaking of nodes confined by the boundary condition), especially earthquakes, and is the most generalized method for seismic design. This method assumes a linear system response and only evaluates the maximum response. Hence, analysis using time integration outlined in sections 5.4.1 and 5.7 is appropriate for problems that have dominant nonlinearity or when results considering the simultaneity of a particular time step are important.

The maximum response is evaluated as a mode combination, which reflects the mode participation rate on the modal response corresponding to the predefined spectrum function. Here, because simultaneity of the modal maximum response is not considered and the response itself is calculated as a combination, the response spectrum analysis results can be seen as an approximate solution for time integration. Hence, if the spectrum function is defined for a particular acceleration or particular seismic wave, the response spectrum analysis result obtains an approximate maximum value of the linear transient response analysis result for the input acceleration. However, the analysis results for seismic design are more generally obtained using the design response spectrum, made from the statistical historical seismic waves in a particular region or country.

#### Modal spectrum response

The static equilibrium equation for response spectrum analysis is shown in equation (5.3.6), and the maximum modal response can be expressed using the spectrum data as follows:

$$\begin{aligned}
 \xi_i^{\max} &= \max[\xi_i(t)] = \Gamma_i S_D(\omega_i, \zeta_i) \\
 \dot{\xi}_i^{\max} &= \max[\dot{\xi}_i(t)] = \Gamma_i S_V(\omega_i, \zeta_i) \\
 \ddot{\xi}_i^{\max} &= \max[\ddot{\xi}_i(t)] = \Gamma_i S_A(\omega_i, \zeta_i)
 \end{aligned} \tag{5.4.14}$$

$S_D(\omega_i, \zeta_i)$  : Displacement spectrum data

$S_V(\omega_i, \zeta_i)$  : Velocity spectrum data

$S_A(\omega_i, \zeta_i)$  : Acceleration spectrum data

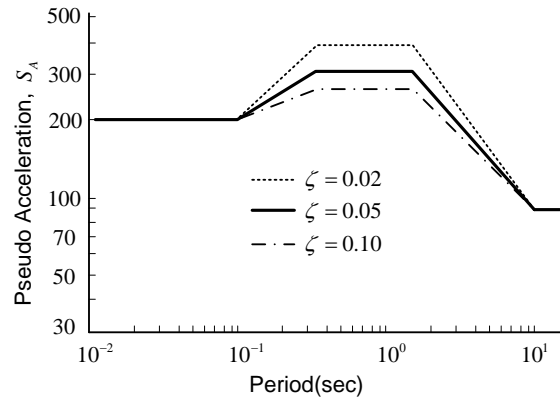
$\Gamma_i$  : Participation factor of the  $i^{\text{th}}$  mode

Substituting equation (5.4.14) into equation (5.3.5) can express the contribution of the maximum modal displacement, velocity, acceleration as an equation of spectral data.

$$\begin{aligned} u_i^{\max} &= \phi_i \Gamma_i S_D(\omega_i, \zeta_i) = \phi_i \Gamma_i S_A(\omega_i, \zeta_i) / \omega_i^2 \\ v_i^{\max} &= \phi_i \Gamma_i S_V(\omega_i, \zeta_i) = \phi_i \Gamma_i S_A(\omega_i, \zeta_i) / \omega_i \\ a_i^{\max} &= \phi_i \Gamma_i S_A(\omega_i, \zeta_i) \end{aligned} \quad (5.4.15)$$

A point in the spectrum data is defined as the absolute maximum modal response value of the natural period (natural frequency), and the effects of the modal damping ratio is included. Because the maximum response of each period is very diverse for the response spectrum of a particular acceleration history, it is expressed as a very complex graph form. However for the design response spectrum, a simple line combination in log scale as shown in figure 5.4.3 is generally used:

Figure 5.4.3 Example of acceleration response spectrum



#### Modal combination method

The maximum physical quantities for each mode (maximum value of each displacement, stress, member force, reaction force etc. component) is called  $R_i^{\max}$ . If the actual maximum physical quantity is assumed as the sum of the maximum values of each mode, simply adding the maximum values of each mode is sufficient. However, because the maximum values of each mode cannot be guaranteed to occur at the same time step, the maximum value cannot be found using only simple linear superposition.

$$R_{\max} \neq \sum_{i=1}^N R_i^{\max} \quad (5.4.16)$$

Hence, a modal combination method needs to be introduced to evaluate the maximum value approximately. Various modal combination methods that consider the superposition characteristics or damping effects have been introduced, but because there is no definite method that gives an appropriate value for all cases, the characteristics of each modal combination method need to be understood.

- Summation of the absolute value (ABS)

$$R_{\max} = \sum_{i=1}^N |R_i^{\max}| \quad (5.4.17)$$

This method assumes that all modal responses have the same phase and judges all absolute maximum modal values to occur at the same time. Hence, it provides the largest value.

- Square root of the summation of the squares (SRSS)

$$R_{\max} = \sqrt{\sum_{i=1}^N (R_i^{\max})^2} \quad (5.4.18)$$

This method provides appropriate results when each mode is sufficiently separated:

- Naval research laboratory method (NRL)

$$R_{\max} = |R_m^{\max}| + \sqrt{\sum_{i=1, i \neq m}^N (R_i^{\max})^2} \quad (5.4.19)$$

This method removes one mode ( $m$ ) that has the maximum absolute value from the SRSS method, and like the SRSS method, this method provides appropriate results when each mode is sufficiently separated.

Because these methods above are effective only when the modes are sufficiently separated and not adjacent, the US Nuclear Regulatory Commission (NRC) regulatory guide 1.92(1976) suggests appropriate evaluation methods for maximum values when multiple modes are adjacent.

- Ten percent method (TENP)

$$R_{\max} = \sqrt{\sum_{i=1}^N \left( R_i^2 + 2 \sum_{j=1}^{i-1} |R_i R_j| \right)} \quad (5.4.20)$$

This method includes effects of all adjacent frequency modes within 10% of the SRSS. Here, the frequencies of two modes  $i, j$  ( $j < i$ ) are judged to be adjacent within 10% frequency if the following condition is satisfied:

$$\frac{\omega_i - \omega_j}{\omega_i} \leq 0.1 \quad (5.4.21)$$

► Complete quadratic combination method (CQC)

$$R_{\max} = \sqrt{\sum_{i=1}^N \sum_{j=1}^i R_i \rho_{ij} R_j} \quad (5.4.22)$$

Here,  $\rho_{ij}$  is the cross-correlation coefficient, which is defined as follows:

$$\rho_{ij} = \frac{8\sqrt{\zeta_i \zeta_j} (\zeta_i + r_{ij} \zeta_m) r_{ij}^{3/2}}{(1 - r_{ij}^2)^2 + 4\zeta_i \zeta_j r_{ij} (1 + r_{ij}^2) + 4(\zeta_i^2 + \zeta_j^2) r_{ij}^2} \quad (5.4.23)$$

$r_{ij}$  : Frequency ratio ( $\omega_j / \omega_i$ ),  $\omega_j < \omega_i$

If  $i = j$  in equation (5.4.23),  $\rho_{ij} = 1$  regardless of the damping ratio. If the damping ratio is '0',  $\rho_{ij} = 1$  for all nodes and the results are the same as the SRSS results. When the damping ratios of two modes are identical, it can be simplified to equation (5.2.24)

$$\rho_{ij} = \frac{8\zeta^2 (1 + r_{ij}) r_{ij}^{3/2}}{(1 - r_{ij}^2)^2 + 4\zeta^2 r_{ij} (1 + r_{ij})^2} \quad (\zeta_i = \zeta_j = \zeta) \quad (5.4.24)$$

#### Sign of modal combination result

Because modal combination methods are displayed as absolute values of the mode results, all response spectrum results always have a positive (+) value. However, for directional results such as reaction force or deformed shape, appropriate signs need to be applied. The most general method for determining the sign of the combined results is following the sign of the major mode. The major mode is defined as the mode, out of the modes that have the largest mass participation rate for each directional component, that has the most closest direction to the defined spectrum direction (load direction).

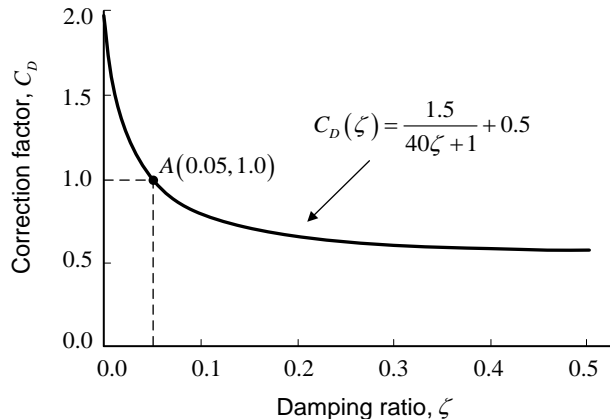
### Spectrum data correction

Spectrum data is a function form for the natural frequency and modal damping ratio, as shown in equation (5.4.14). However, because the user cannot know the frequency before analysis, the spectrum data is defined as a table with a constant interval. Hence, the interpolation is used when reading the spectrum value of the applicable frequency or period of the structure and linear interpolation on a logarithmic scale, which expresses the spectrum response for natural period change, is most generally used. When entering the spectrum data for multiple damping ratios, linear interpolation on a logarithmic scale is performed in the same way for the structural modal damping ratio.

However when spectrum data is available for only one damping ratio, there is no data for interpolation and a special interpolation method is needed for that single damping ratio. The Japan specifications for highway bridges (2002) suggest the following correction factor for the damping ratio:

$$C_D(\zeta) = \frac{1.5}{40\zeta + 1} + 0.5 \quad (5.4.25)$$

Figure 5.4.4 Correction factor for damping ratio



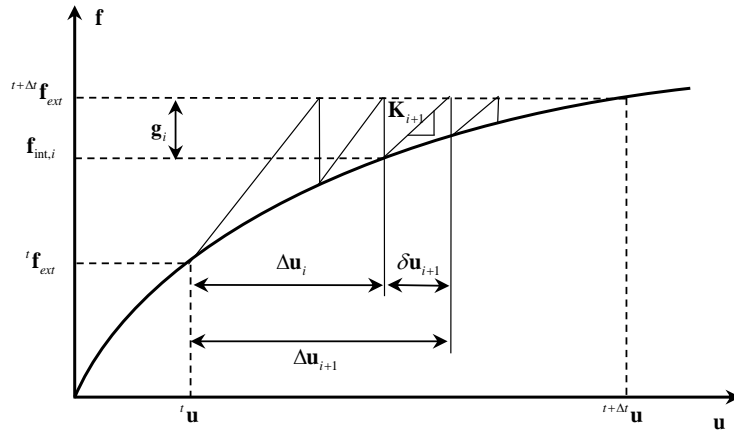
When the damping ratio is '0.05',  $C_D = 1$  (Point A) and equation (5.4.25) denotes the correction factor when the damping ratio of the spectrum data is '0.05'. Hence, when the damping ratio ( $\zeta_{\text{spectrum}}$ ) of the spectrum data is not '0.05', the ratio of correction factors corresponding to each damping is applied as the final damping correction factor, as shown in equation (5.4.26).

$$\bar{R}_i^{\max} = \frac{C_D(\zeta_i)}{C_D(\zeta_{\text{spectrum}})} R_i^{\max} \quad (5.4.26)$$

# Section 5 Nonlinear Finite Element Solution

Nonlinear Finite Element Solution is a method of converging the accumulated incremental solution from iterative calculations to the correct solution, and it is processed as shown in figure 5.5.1.

Figure 5.5.1 Accumulated incremental solution and nonlinear finite element convergence



In the figure,  $f_{ext}^t$  and  $f_{ext}^{t+\Delta t}$  each represent the external forces at time  $t$  and time  $t + \Delta t$ , and the solution and incremental solution between time  $t$  and time  $t + \Delta t$  can be expressed as the following relationship:

$${}^{t+\Delta t}\mathbf{u} = {}^t\mathbf{u} + \Delta\mathbf{u} \tag{5.5.1}$$

$\Delta\mathbf{u}$  : Incremental solution occurring at time increment  $\Delta t$

If iterative calculation is performed for nonlinear analysis in the time increment  $\Delta t$ , the accumulated incremental solution is as follows:

$$\Delta\mathbf{u} = \sum_{i=1}^n \delta\mathbf{u}_i \quad \text{or} \quad \Delta\mathbf{u}_{i+1} = \Delta\mathbf{u}_i + \delta\mathbf{u}_{i+1} \tag{5.5.2}$$

$\Delta\mathbf{u}_i$  : Accumulated incremental solution up to  $i$  th iterative calculation

$\delta\mathbf{u}_{i+1}$  : Incremental solution occurring at  $i+1$  th iterative calculation

$\delta \mathbf{u}_{i+1}$  is calculated from the following linear simultaneous equation using the tangential stiffness matrix  $\mathbf{K}_{i+1}$ .

$$\delta \mathbf{u}_{i+1} = \mathbf{K}_{i+1}^{-1} \mathbf{g}_i \quad (5.5.3)$$

$\mathbf{g}_i$  : Residual force, unbalanced force

The unbalanced force  $\mathbf{g}_i$  is expressed as the following difference between external force  ${}^{i+\Delta t} \mathbf{f}_{ext}$  and internal force  $\mathbf{f}_{int,i}$ .

$$\mathbf{g}_i = {}^{i+\Delta t} \mathbf{f}_{ext} - \mathbf{f}_{int,i} \quad (5.5.4)$$

Equations (5.5.2)-(5.5.4) are iterated until it satisfies the user specified convergence criteria, and the convergence criteria judges using the change in member force, displacement or energy etc.

#### Line search

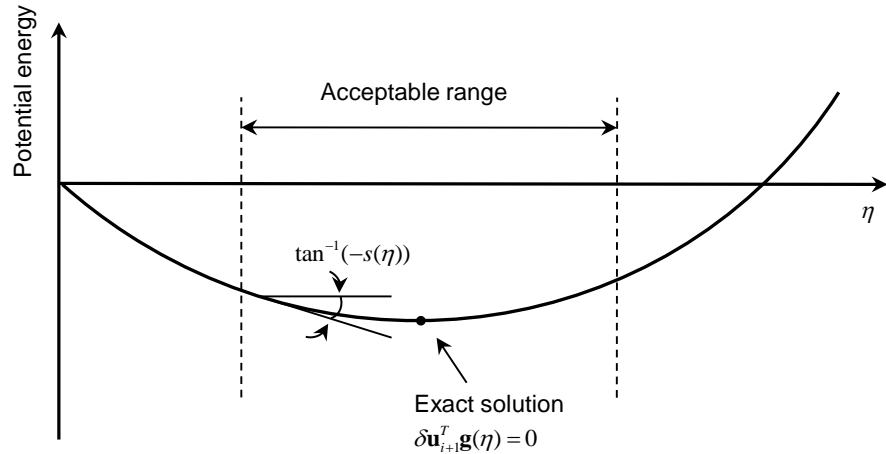
GTS NX provides the line search function to improve the performance of the basic iterative solutions explained above. The fundamental concept of line search is the introduction of a scalar value  $\eta$  during the process of adding the calculated incremental solution  $\delta \mathbf{u}_{i+1}$  to the accumulated incremental solution for improved accuracy. In this case, the accumulated incremental solution is calculated as follows:

$$\Delta \mathbf{u}_{i+1} = \Delta \mathbf{u}_i + \eta \delta \mathbf{u}_{i+1} \quad (5.5.5)$$

Assuming that the calculated  $\Delta \mathbf{u}_{i+1}$  above satisfies the equilibrium state and uses the principal of stationary total potential energy, the line search problem results in finding the  $\eta$  at which the derivative of the total potential energy for  $\eta$  is '0'.

$$s(\eta) = \delta \mathbf{u}_{i+1}^T \mathbf{g}(\eta) = 0 \quad (5.5.6)$$

Figure 5.5.2 Conceptual diagram of line search algorithm



Assuming linear change for the energy derivative  $s(\eta)$  about  $\eta$ , the  $\eta$  that satisfies equation (5.5.6) is calculated as follows:

$$\eta = \frac{-s(\eta = 0)}{s(\eta = 1) - s(\eta = 0)} \quad (5.5.7)$$

Here, the slopes at which  $\eta$  is '0' or '1' can be expressed as follows:

$$\begin{aligned} s(\eta = 0) &= \delta \mathbf{u}_{i+1}^T \mathbf{g}_i \\ s(\eta = 1) &= \delta \mathbf{u}_{i+1}^T \mathbf{g}_{i+1} \end{aligned} \quad (5.5.8)$$

Because the assumptions made for the line search algorithm are not accurately satisfied for the real case, the  $s(\eta)$  calculated from equation (5.5.7) is generally not '0'. In GTS NX the processes outlined above are repeated until the  $s(\eta_j) / s(\eta = 0)$  value is below the user-specified constant value.

#### Initial stiffness, Newton Raphson, Modified Newton Raphson

The iterative methods in nonlinear analysis can be classified into the Initial stiffness, Newton Raphson, Modified Newton Raphson methods depending on the calculation point of the tangential stiffness. The Initial stiffness method continuously maintains the tangential stiffness calculated at the start point of analysis. The Newton Raphson method recalculates the tangential stiffness for each iterative calculation. The Modified Newton Raphson calculates the tangential stiffness where a change in external force occurs. Because tangential stiffness, matrix calculation, and matrix decomposition requires a long calculation time, using the Initial stiffness and Modified Newton Raphson methods is

faster than the Newton Raphson method when problems do not occur in the convergence process. GTS NX does not classify the Initial stiffness and Modified Newton Raphson methods explicitly. Defining the tangential stiffness recalculation point can give the effects of all iterative methods.

#### Automatic stiffness matrix recalculation

It is important to select an appropriate calculation point for tangential stiffness, depending on the characteristics of the target analysis model such as nonlinearity, evenness of the converging solution, etc. GTS NX provides the automatic tangential stiffness update, which judges an appropriate recalculation point by considering the overall characteristics of the nonlinear problem such as convergence characteristics or determination of divergence etc., as a nonlinear finite element solution. Tangential stiffness update is performed when the following conditions are satisfied:

- ▶ When the expected number of iterative calculations is larger than the user defined maximum number
- ▶ When the solution is determined to diverge

#### Convergence condition

The convergence of the iterative solution is judged using the force norm, displacement norm and energy norm.

$$\text{Force norm ratio} = \frac{\sqrt{\mathbf{g}_i^T \mathbf{g}_i}}{\sqrt{\Delta \mathbf{f}_{int,i}^T \Delta \mathbf{f}_{int,i}}} \quad (5.5.9)$$

$$\text{Displacement norm ratio} = \frac{\sqrt{\delta \mathbf{u}_i^T \delta \mathbf{u}_i}}{\sqrt{\Delta \mathbf{u}_i^T \Delta \mathbf{u}_i}} \quad (5.5.10)$$

$$\text{Energy magnitude ratio} = \left| \frac{\delta \mathbf{u}_i^T \mathbf{g}_i}{\Delta \mathbf{u}_i^T \Delta \mathbf{f}_{int,i}} \right| \quad (5.5.11)$$

For general nonlinear systems, all convergence norms decrease simultaneously as the system converges. Particularly, the force norm represents the size of the unbalanced force and has the closest relationship with the degree of satisfaction of the nonlinear equation. On the other hand, the displacement norm represents the size of the incremental solution and is not appropriate as a single convergence norm for problems with a very large local stiffness, such as for systems using the penalty method.

GTS NX compares a single or multiple norms out of these three norms to the user-provided tolerance to determine convergence.

#### Divergence determination and load bisection

Determining the divergence for a solution is an important criterion used in automatic tangential stiffness update, and the divergence rate  $E_i$  is determined fundamentally.

$$E_i = \frac{\delta \mathbf{u}_i^T \mathbf{g}_i}{\delta \mathbf{u}_i^T \mathbf{g}_{i-1}} \quad (5.5.12)$$

When the absolute value of the divergence rate is larger than '1' ( $|E_i| \geq 1$ ), the nonlinear analysis solution is judged to have possible divergence and necessary measures are taken on the algorithm, such as recalculation of the stiffness matrix or load bisection.

Load bisection is applied when the increment of the current load step is too large to obtain a converging solution, such as when the solution diverges or when the number of required iterative calculations is larger than the user defined maximum number etc. By restarting the iterative calculation through bisecting the current load increment, an inappropriate load increment size can be dealt with flexibly. GTS NX performs load bisection automatically until the user defined maximum bisection level is reached.

#### Automatic time increment adjustment

To increase the efficiency of nonlinear analysis, GTS NX includes a function that automatically adjusts the time increment size as the base of the nonlinear analysis astringency. The fundamental time increment size and maximum increment size is determined by the user input. When using the automatic time increment adjustment function in nonlinear analysis, the time increment size of a particular time step increases or decreases based on the number of iterative calculations needed for convergence in the previous increment step.

$$\Delta t^{i+1} = n_s \Delta t^i \quad (1 \leq n_s \leq n_{s,\max}) \quad (5.5.13)$$

Here, the increment adjustment factor ( $n_s$ ) is limited to natural numbers to obtain the maximum number of nonlinear solutions in the user intended point or load size. The increment adjustment factor has a range from the minimum value '1' representing the initial increment, and the maximum value ( $n_{s,\max}$ ) provided by the user.

#### Quasi-Newton method

The quasi-Newton method is a type of nonlinear solution is the generalized form of the secant method. It maintains the advantages of the Modified Newton Raphson method, which recomposes the stiffness matrix only when a load increment is present, and improves the problem of low astringency. In other words, costs do not occur for recomposition during iterative calculation of the stiffness matrix and effective calculation using the decomposed stiffness is possible. At the same time, this method can be used to improve the astringency and general performance.

GTS NX uses the BFGS (Broyden-Fletcher-Goldfarb-Shanno) method<sup>6</sup>, a type of quasi-Newton method. The inverse matrix of the stiffness matrix from iterative calculations in nonlinear finite element analysis is adjusted by the following BFGS update process.

$$\mathbf{K}_j^{-1} = \Gamma_j^T \mathbf{K}_{j-1}^{-1} \Gamma_j + z_j \delta_j \delta_j^T \quad (5.5.14)$$

Here,  $j$  represents the BFGS update index, and matrix  $\Gamma_j$  and scalar  $z_j$  can be expressed as follows.

$$\begin{aligned} \Gamma_j &= \mathbf{I} - z_j \gamma_j \delta_j^T \\ z_j &= \frac{1}{\delta_j^T \gamma_j} \end{aligned} \quad (5.5.15)$$

Also, the quasi-Newton vectors  $\delta_j$  and  $\gamma_j$  are expressed using the increment solution  $\delta \mathbf{u}_i$ , which applies the line search factor  $\eta$  from the  $i$ th iterative calculation, and the difference between unbalanced forces during iterative calculation as follows.

$$\begin{aligned} \delta_j &= \Delta \mathbf{u}_i - \Delta \mathbf{u}_{i-1} = \eta \delta \mathbf{u}_i \\ \gamma_j &= \mathbf{g}_i - \mathbf{g}_{i-1} \end{aligned} \quad (5.5.16)$$

The  $i$ th incremental solution during iterative calculations is calculated using the  $j$ th BFGS updated stiffness matrix and unbalanced forces, as shown below:

$$\delta \mathbf{u}^i = \mathbf{K}_j^{-1} \mathbf{g}^{i-1} = \Gamma_j^T \mathbf{K}_{j-1}^{-1} \Gamma_j \mathbf{g}^{i-1} - z_j \delta_j \delta_j^T \mathbf{g}^{i-1} \quad (5.5.17)$$

The inverse matrix of the stiffness matrix is not actually modified by the BFGS update process; the incremental solution is calculated during iterative calculations using a recursive method. In other words, it maintains the decomposed form of the initial stiffness matrix with no BFGS updates. The incremental solution can be found using simple recursive vector operations. The quasi-Newton vector is saved for these operations. The saved vector is erased when incremental analysis converges and the stiffness matrix is recomposed.

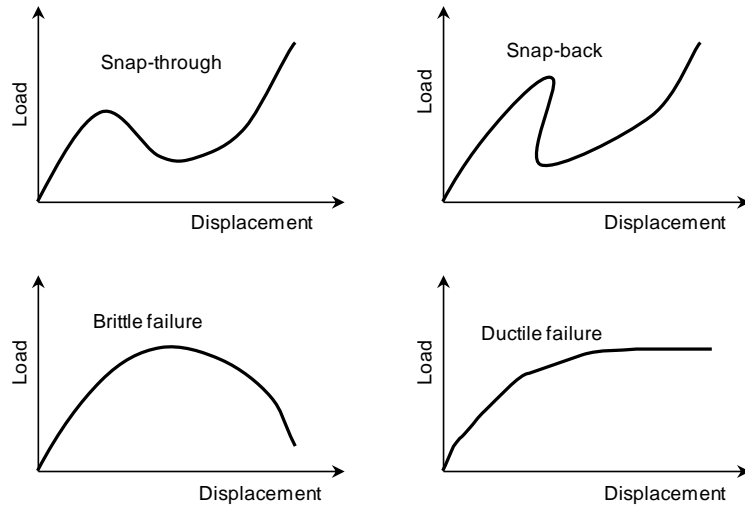
#### Arc-length method

Figure 5.5.3 displays the various displacement load paths, including the unstable equilibrium path. When performing static nonlinear analysis for these phenomena, analysis of the unstable static equilibrium state after the limit point cannot be performed when the general load controlled nonlinear

<sup>6</sup> Matthies, H. and Strang, G., "The solution of nonlinear finite element equations," International Journal for Numerical Methods in Engineering, Vol. 14, Issue 11, pp. 1613-1626, 1979

solution is used. In other words, general nonlinear solutions cannot find the converging solution after the limit point. When using the displacement controlled method, the analyzable region increases locally, but this is not a general solution and tracing is impossible for the snap-back phenomenon. In this case, the arc-length method can be used. The arc-length method can successfully trace the equilibrium path even when the static equilibrium state includes an unstable region.

Figure 5.5.3 Various unstable equilibrium paths



The external forces in the arc-length method are assumed to be proportional to the load parameter  $\lambda$ , which is an independent scalar variable. Hence, the arc-length method can be seen to increase the DOF of the fundamental finite element problem by '1'. However, because the algorithm is composed such that the parameter  $\lambda$  and accumulated incremental solution satisfy the arc-length constraint, the final number of DOF is maintained. The unbalanced forces including the load parameter can be expressed as follows:

$$\mathbf{g}_i(\mathbf{u}_i, \lambda_i) = \lambda_i \mathbf{f}_{ext} - \mathbf{f}_{int,i} \quad (5.5.18)$$

Here, linearizing the condition that the unbalanced forces that occur at the  $i+1$  th iterative calculations due to the incremental solution  $\delta \mathbf{u}_{i+1}$  and incremental load parameter  $\delta \lambda_{i+1}$  is 0. The relationship between the incremental solution and incremental load parameter can be obtained as follows:

$$\delta \mathbf{u}_{i+1} = \mathbf{K}_{i+1}^{-1} (\mathbf{g}_i + \delta \lambda_{i+1} \mathbf{f}_{ext}) \quad (5.5.19)$$

Using this, the accumulated incremental solution at the  $i+1$  th iterative calculation is as follows:

$$\Delta \mathbf{u}_{i+1} = \Delta \mathbf{u}_i + \delta \bar{\mathbf{u}} + \delta \lambda_{i+1} \mathbf{u}_T \quad (5.5.20)$$

$\delta \bar{\mathbf{u}} = \mathbf{K}_{i+1}^{-1} \mathbf{g}_i$  : Incremental solution for unbalanced force

$\mathbf{u}_T = \mathbf{K}_{i+1}^{-1} \mathbf{f}_{ext}$  : Displacement generated for total external force

GTS NX uses the Crisfield, Riks, or Modified Riks method arc-length constraints. The Crisfield method<sup>7</sup> is used as the default arc-length constraint:

$$\Delta \mathbf{u}_{i+1}^T \Delta \mathbf{u}_{i+1} = \Delta l^2 \quad (5.5.21)$$

$\Delta l$  : Arc-length

The incremental load parameter  $\delta \lambda_{i+1}$  can be calculated from the equation above, and substituting this can calculate the  $i + 1$  th iterative calculation solution. Like the general nonlinear solution, this process is repeated until the user specified convergence criteria is satisfied and the convergence criteria are the same as that of the general nonlinear solution. In other words, convergence is judged using the change in member force, displacement, or energy.

When using the arc-length method, accurate load state calculation can be difficult because the load increment is determined by the arc-length constraint condition and cannot be controlled by the user. Hence, the applicable range of the arc-length method is limited to problems that need tracing of the unstable equilibrium state. No additional advantages exist for general nonlinear problems.

#### Over-relaxation method

The over-relaxation method is one of the methods to improve the convergence rate by multiplying the estimated unbalance force by the coefficient at the iterative calculation.

Although it is a basic approach rather than a line search method, it is a method that is very similar to the initial stiffness method because the formula is very simple and unlike the line search method, the additional analysis time is required in the iterative calculation.

$$\mathbf{K}_e \Delta \mathbf{u}_i = \mathbf{K}_e \Delta \mathbf{u}_{i-1} + \omega \mathbf{r}(\Delta \mathbf{u}_{i-1}) \quad (5.5.22)$$

Where  $\omega$  is the excess relaxation coefficient.

<sup>7</sup> Crisfield, M.A., "An arc-length method including line searches and accelerations," International Journal for Numerical Methods in Engineering, Vol. 19, Issue 9, pp 1269-1289, 1983

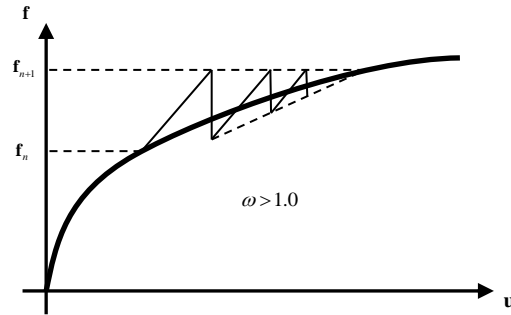


Figure 5.5.4 Over-relaxation method

The initial relaxation coefficient is directly input by the user, 1.2 is defined as the default value, and should not exceed 2.0 at maximum.

#### Enhanced predictor

The initial displacement estimation method is a method of predicting the initial displacement at the present stage using the load factor ratio taken from the present stage divided by previous stage and multiplied by the displacement result of the previous stage as shown in the following equation.

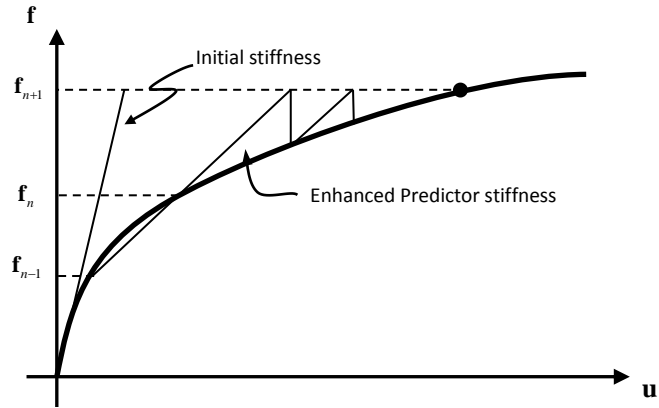
$$\Delta \mathbf{u}_n^{predictor} = \frac{\Delta \mu_n}{\Delta \mu_{n-1}} \Delta \mathbf{u}_{n-1} \quad (5.5.23)$$

The estimated displacements do not exactly coincide with those of the current step, but they are useful for iterative calculations because they predict closer results than the displacements estimated by elastic stiffness.

Particularly, it is more effective when the material model has a large plasticity. However, because it is less accurate than the estimated tangent stiffness by Newton-Raphson, it is recommended to use it with the initial stiffness method.

In general, the initial stiffness method is a stable method for solving the problem.

Figure 5.5.5 Estimation of Initial Deformation (enhanced predictor)



## Section 6

# Strain/Stress Measurement Considering Large Deformation

For geometric linear analysis, the strain and stress are defined without considering the shape difference before and after deformation. The strain in geometric linear analysis is generally defined as follows:

$$\boldsymbol{\varepsilon} = \frac{1}{2} \left[ \frac{\partial \mathbf{u}}{\partial \mathbf{X}} + \left( \frac{\partial \mathbf{u}}{\partial \mathbf{X}} \right)^T \right] \quad (5.6.1)$$

$\mathbf{u}$  : Displacement

$\mathbf{X}$  : Coordinates before or after deformation

For geometric nonlinear analysis that considers large deformation, the strain can be defined using various methods and a corresponding stress exists for each strain to define virtual work.

### Definition of strain

Strains that consider large deformations include Green strain, Green-Lagrange strain and rate of deformation or strain rate. The Green strain tensor  $\mathbf{E}$  is defined as follows:

$$ds^2 - dS^2 = 2d\mathbf{X} \cdot \mathbf{E} \cdot d\mathbf{X} \quad (5.6.2)$$

$\mathbf{X}$  : Coordinates of a particular position on the structure before deformation

The Green strain can be seen as the difference between the squared value of the differential length before deformation  $dS$  and after deformation  $ds$ . The Green strain tensor can be defined using the deformation gradient as follows:

$$\mathbf{E} = \frac{1}{2} (\mathbf{F}^T \cdot \mathbf{F} - \mathbf{I}) \quad (5.6.3)$$

If only rigid motion occurs, Green strain does not occur and it is appropriate as a measurement of deformation.

The rate of deformation  $\mathbf{D}$  is defined by the velocity gradient as follows:

$$\mathbf{D} = \frac{1}{2}(\mathbf{L} + \mathbf{L}^T) = \text{sym}\left[\frac{\partial \mathbf{v}}{\partial \mathbf{x}}\right] \quad (5.6.4)$$

$\mathbf{v}$  : Velocity vector

$\mathbf{X}$  : Coordinates of a particular position on the structure before deformation

In other words, it corresponds to the symmetric part of the velocity gradient tensor. The rate of deformation can be seen as a value for the squared differential length.

$$\frac{\partial ds^2}{\partial t} = 2d\mathbf{x} \cdot \mathbf{D} \cdot d\mathbf{x} \quad (5.6.5)$$

The rate of deformation also does not occur when only rigid motion exists, and it has the following relationship with the Green strain:

$$\mathbf{D} = \mathbf{F}^{-T} \cdot \dot{\mathbf{E}} \cdot \mathbf{F}^{-1} \quad (5.6.6)$$

Because the rate of deformation is a rate of change with time, it is generally time integrated and used as a strain. If analysis that considers geometric nonlinearity of a material is performed in GTS, NX the strain is computed by time integrating the rate of deformation. GTS NX uses the rate of deformation or strain rate.

#### Definition of stress

When geometric deformation is large, the stress can also be defined using various methods. GTS NX uses the Cauchy stress.

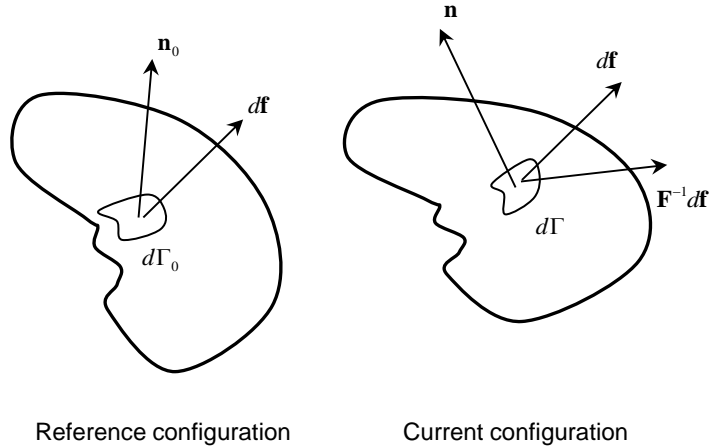
Because Cauchy stress is a value that satisfies the equilibrium equation of the current shape, it is also known as true stress  $\boldsymbol{\sigma}$  and is defined as follows:

$$\mathbf{n} \cdot \boldsymbol{\sigma} \cdot d\Gamma = d\mathbf{f} = t d\Gamma \quad (5.6.7)$$

The Cauchy stress of the shape before deformation can be converted to the 2nd PK stress (Piola-Kirchhoff:  $\mathbf{S}$ ) as follows:

$$\mathbf{S} = J\mathbf{F}^{-1} \cdot \boldsymbol{\sigma} \cdot \mathbf{F}^{-T} \quad (5.6.8)$$

Figure 5.6.1 Shape before/after deformation and force direction for defining stress



The physical meaning of 2nd PK stress is not clear, but it is useful in describing the equation of motion when coupled with the Green strain and so it is often used to define the behavior of materials with an energy potential such as rubber. GTS NX uses the following stress and strain integration method for all materials:

#### Stress rate and strain rate integration

Elasto-plastic materials, viscoelastic materials etc. do not have energy potential, but use a constitutive relationship consisting of the strain rate and objective stress rate. The Jaumann stress rate used is defined as follows:

$$\dot{\sigma}^J = \dot{\sigma} - \mathbf{w} \cdot \sigma - \sigma \cdot \mathbf{w}^T \quad (5.6.9)$$

Strain rate and objective stress rate have the following relationship from the constitutive equation of the material:

$$\dot{\sigma}^J = \mathbf{C} : \mathbf{D} \quad (5.6.10)$$

Reflecting the central difference and considering the structural rotation in equation (5.6.10), the equation that calculates the stress at step  $n+1$  using the stress and strain increments calculated at step  $n$ :

$$\sigma_{n+1} = \Delta \mathbf{R} \cdot \sigma_n \cdot \Delta \mathbf{R}^T + \mathbf{C} : \Delta \epsilon \quad (5.6.11)$$

The rotation amount increment  $\Delta \mathbf{R}$  is calculated as follows<sup>8</sup> to satisfy the incrementally objective stress condition.

$$\Delta \mathbf{R} = (\mathbf{I} - \frac{1}{2} \Delta \mathbf{W})^{-1} (\mathbf{I} + \frac{1}{2} \Delta \mathbf{W}) \quad (5.6.12)$$

Particularly, the strain increment and incremental spin calculation is performed on the  $n+1/2$  shape.

$$\Delta \boldsymbol{\varepsilon} = \frac{1}{2} \left( \frac{\partial \Delta \mathbf{u}}{\partial \mathbf{x}_{n+1/2}} + \left[ \frac{\partial \Delta \mathbf{u}}{\partial \mathbf{x}_{n+1/2}} \right]^T \right), \quad \Delta \boldsymbol{\omega} = \frac{1}{2} \left( \frac{\partial \Delta \mathbf{u}}{\partial \mathbf{x}_{n+1/2}} - \left[ \frac{\partial \Delta \mathbf{u}}{\partial \mathbf{x}_{n+1/2}} \right]^T \right) \quad (5.6.13)$$

The strain rate integral is also calculated using equation (5.6.11) and uses the structural rotation amount increment  $\Delta \mathbf{R}$ .

<sup>8</sup> Hughes, T.J.R. and Winget, J., "Finite rotation effects in numerical integration of rate constitutive equations arising in large deformation analysis," International Journal for Numerical Methods in Engineering, Vol. 15, 1980

## Section 7

## Nonlinear Dynamic Response

GTS NX supports nonlinear time history analysis that includes geometric, material nonlinearity and it is based on implicit time integration.

## 7.1

Implicit Time  
Integration

The dynamic equilibrium equation in nonlinear time history analysis uses the  $\text{HHT}-\alpha$  method as implicit time integration, just like for linear time history analysis, and uses the following modified equilibrium equation.

$$\frac{\partial}{\partial t}(\mathbf{M}\mathbf{v}^{n+1}) + (1 + \alpha_H)[\mathbf{C}\mathbf{v}^{n+1} + \mathbf{f}^{\text{int},n+1} - \mathbf{f}^{\text{ext},n+1}] - \alpha_H[\mathbf{C}\mathbf{v}^n + \mathbf{f}^{\text{int},n} - \mathbf{f}^{\text{ext},n}] = \mathbf{0} \quad (5.7.1)$$

In nonlinear time history analysis, the effects of the mass matrix rotation due to geometric nonlinearity are considered. The rotational inertia part of the mass matrix is modified for each iterative calculation, according to the finite rotation of the nodes, and the inertial force generated from the rate of change of the mass matrix is considered in analysis.

Nonlinear time history analysis calculates the convergence solution for each time step using the nonlinear finite element solution in section 5.5. The unbalanced forces are expressed from equation (5.7.1) as follows:

$$\mathbf{g}_{n+1} = \frac{\partial}{\partial t}(\mathbf{M}^{n+1}\mathbf{v}^{n+1}) + (1 + \alpha_H)[\mathbf{C}^{n+1}\mathbf{v}^{n+1} + \mathbf{f}^{\text{int},n+1} - \mathbf{f}^{\text{ext},n+1}] - \alpha_H[\mathbf{C}^{n+1}\mathbf{v}^n + \mathbf{f}^{\text{int},n} - \mathbf{f}^{\text{ext},n}] \quad (5.7.2)$$

The tangential stiffness matrix can be found by applying the time step equation (5.4.3), from the Newmark method for velocity and acceleration, onto the unbalanced force and differentiating for the displacement DOF, as follows:

$$\mathbf{A} = \frac{1}{\beta\Delta t^2}\mathbf{M}^{n+1} + \frac{\gamma}{\beta\Delta t}\dot{\mathbf{M}}^{n+1} + \frac{(1 + \alpha_H)\gamma}{\beta\Delta t}\mathbf{C}^{n+1} + (1 + \alpha_H)\frac{\partial\mathbf{f}^{\text{int},n+1}}{\partial\mathbf{u}} - (1 + \alpha_H)\frac{\partial\mathbf{f}^{\text{ext},n+1}}{\partial\mathbf{u}} \quad (5.7.3)$$

Here,  $\alpha_H = -0.05$  is used as the default value, just like linear time history analysis. Also, to secure unconditional stability, the following values are used :  $\gamma = (1 - 2\alpha_H) / 2$  ,  $\beta = (1 - \alpha_H)^2 / 4$

**Angular velocity and angular acceleration**

When considering geometric nonlinearity in nonlinear time history analysis, the angular velocity and angular acceleration need to be updated by reflecting the effects of body axis system rotation. Defining

the body axis system where finite rotation occurs as  $\phi$ , the Newmark time step equation in the coordinate system of the body axis system is as follows:

$$\boldsymbol{\omega}_\phi^{n+1} = \boldsymbol{\omega}_\phi^n + \Delta t \left[ \gamma \boldsymbol{\alpha}_\phi^{n+1} + (1-\gamma) \boldsymbol{\alpha}_\phi^n \right] \quad (5.7.4)$$

$\boldsymbol{\omega}_\phi, \boldsymbol{\alpha}_\phi$  : Angular velocity and angular acceleration about the body axis system  $\phi$

Using the base vector perpendicular to the body axis system  $\mathbf{e}_\phi$ , the equation above can be expressed for the GCS.

$$\boldsymbol{\omega}^{n+1} = \Delta t \gamma \boldsymbol{\alpha}^{n+1} + \left( \mathbf{e}_\phi^{n+1} \mathbf{e}_\phi^n \right) \left[ \boldsymbol{\omega}^n + \Delta t (1-\gamma) \boldsymbol{\alpha}^n \right] \quad (5.7.5)$$

The product of the perpendicular base vectors in equation (5.7.5) is the same as the incremental rotation matrix found below:

$$\Delta \mathbf{C} = \exp(\Delta \hat{\theta}) \quad (5.7.6)$$

$\Delta \hat{\theta}$  : Skew symmetric matrix for the rotation amount increment

The rotation amount increment can be expressed by the Newmark method using the incremental rotation matrix, as shown below.

$$\Delta \boldsymbol{\theta} = \Delta t^2 \beta \boldsymbol{\alpha}^{n+1} + \Delta \mathbf{C} \left[ \Delta t \boldsymbol{\omega}^n + \Delta t^2 \left( \frac{1}{2} - \beta \right) \boldsymbol{\alpha}^n \right] \quad (5.7.7)$$

Rearranging equation (5.7.7) for angular velocity and angular acceleration respectively and substituting into equation (5.7.5) gives the following updating equations for both angular velocity and angular acceleration.

$$\begin{aligned} \boldsymbol{\omega}^{n+1} &= \frac{\gamma}{\Delta t \beta} \Delta \boldsymbol{\theta} + \Delta \mathbf{C} \left[ \left( 1 - \frac{\gamma}{\beta} \right) \boldsymbol{\omega}^n + \Delta t \left( 1 - \frac{\gamma}{2\beta} \right) \boldsymbol{\alpha}^n \right] \\ \boldsymbol{\alpha}^{n+1} &= \frac{1}{\Delta t^2 \beta} \Delta \boldsymbol{\theta} + \Delta \mathbf{C} \left[ \frac{1}{\Delta t \beta} \boldsymbol{\omega}^n + \left( 1 - \frac{1}{2\beta} \right) \boldsymbol{\alpha}^n \right] \end{aligned} \quad (5.7.8)$$

**Damping effect**

Mass proportional damping and stiffness proportional damping are also considered in nonlinear time history analysis, just like linear time history analysis. In this case, the damping matrix is composed similarly to equation (5.4.5). The mass matrix, which is used to calculate the damping matrix in nonlinear time history analysis, considers the rotational effects due to finite rotations and the stiffness matrix only uses the stiffness matrix due to material nonlinearity.

$$\mathbf{C} = \alpha_j^e \mathbf{M}_j^e + \beta_j^e \mathbf{K}_{mat,j}^e + \mathbf{B} \quad (5.7.9)$$

$\mathbf{K}_{mat}$  : Stiffness matrix due to material nonlinearity

## Section 8 Contact Condition

Contact analysis fundamentally assumes that two objects in a space can be in contact, but cannot penetrate each other (non-penetration condition), and is nonlinear in behavior or in condition from a physical point of view. The type of contacts are general contact (considers the impact and impact friction between two objects in analysis) and rough contact (does not consider sliding) shown in figure 5.8.1, and welded contact (two objects are welded from the start of analysis) shown in figure 5.8.2. Here, the welded contact is assigned depending on the position of two objects at the start of analysis and can be seen as linear.

Figure 5.8.1 Concept of general contact and rough contact

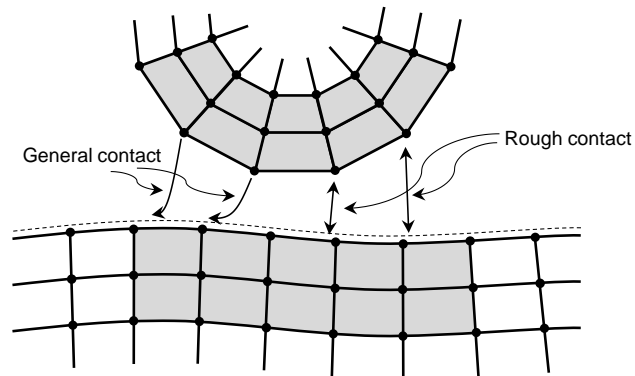
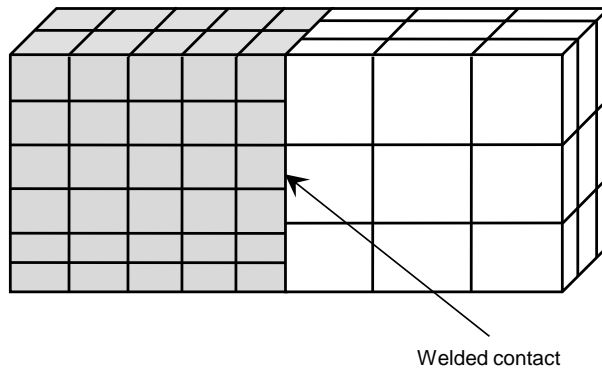


Figure 5.8.2 Concept of welded contact



**Relationship between contact condition and analysis type**

The contact condition can be used for initially adjacent bodies in structural analysis, consolidation analysis and seepage analysis.

The contact can be classified with the node-to-surface contact, or surface-to-surface contact. Node-to-surface contact takes less time, but the solution accuracy is relatively low because the nodes of the main object tend to penetrate through the sub object. On the other hand, surface-to-surface contact takes longer but the non-penetrating conditions are satisfied relatively accurately, allowing the accurate simulation of the structural behavior. GTS NX supports the surface-to-surface contact.

The general contact can be used in nonlinear structural analysis (static, dynamic) and consolidation analysis. The general contact corresponds to the nonlinear condition, and its behavior is different according to the geometric nonlinearity consideration in terms of analysis techniques. In case of considering geometric nonlinearity, the possibility of contact is considered for all master segments under the assumption of large displacement. On the other hand, only the contact closed to within initial user-defined distance between master segment and slave node is considered.

**Contact plane search**

Contact search uses the slave node/master segment algorithm. This algorithm determines contact by the adjacency between the slave node and master segment, or how much the slave node penetrates the master segment. Generally, the order of the slave node defined object and master segment defined object does not matter. But from a numerical point of view, the master segment needs to be defined on the object with a relatively larger stiffness, or relatively element-sparse object, to obtain more accurate analysis results.

To determine the actual contact of the slave node and master segment, the global search process is conducted. Global search is the process that determines the preliminary slave nodes where objects or segments can collide in space. Contact search is performed locally for the slave node and master segment sets determined by global search.

To determine whether nodes and planes are actually in contact, the slave nodes need to be projected orthogonally on the master segment as shown in figure 5.8.3. Defining vector  $\mathbf{r}$  from the origin to the projected point (A), and vector  $\mathbf{x}_s$  from the origin to the slave node gives the following equation:

$$\begin{aligned} \frac{\partial \mathbf{r}(\xi_c, \eta_c)}{\partial \xi} \cdot [\mathbf{x}_s - \mathbf{r}(\xi_c, \eta_c)] &= 0 \\ \frac{\partial \mathbf{r}(\xi_c, \eta_c)}{\partial \eta} \cdot [\mathbf{x}_s - \mathbf{r}(\xi_c, \eta_c)] &= 0 \end{aligned} \quad (5.8.1)$$

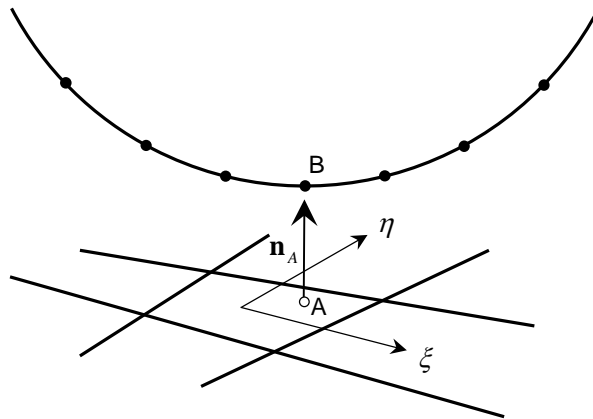
Here,  $(\xi_c, \eta_c)$  is the position of contact point (A) on the master segment, expressed in the natural coordinate system. The  $(\xi_c, \eta_c)$  that satisfies the equation above can be calculated numerically using

the Newton-Raphson method. The coordinate increment  $(\Delta\xi_c, \Delta\eta_c)$  for applying the Newton-Raphson method is as follows:

$$\begin{bmatrix} \frac{\partial \mathbf{r}}{\partial \xi} \\ \frac{\partial \mathbf{r}}{\partial \eta} \end{bmatrix} \begin{bmatrix} \frac{\partial \mathbf{r}}{\partial \xi} & \frac{\partial \mathbf{r}}{\partial \eta} \end{bmatrix} \begin{Bmatrix} \Delta\xi \\ \Delta\eta \end{Bmatrix} = \begin{bmatrix} \frac{\partial \mathbf{r}}{\partial \xi} \\ \frac{\partial \mathbf{r}}{\partial \eta} \end{bmatrix} \{ \mathbf{r}(\xi_c, \eta_c) - \mathbf{x}_s \} \quad (5.8.2)$$

Using the initial condition as  $(\xi_c, \eta_c) = (0, 0)$ , the equation above converges easily when the position of contact point (A) or slave node (B) is not far from the master segment. If the next slave node is checked and determined to have penetrated the contact plane, the force (contact force) proportional to the penetration depth is added to the slave node and contact plane.

Figure 5.8.3 Normal relationship between slave node and master segment



#### Calculation of contact force

The displacement relationship between the slave node and master segment, which are determined to be in contact, is confined using the penalty method. In GTS NX, the gap and contact force is defined using the following equations (5.8.3), (5.8.4):

$$g_N = (\mathbf{x}^B - \mathbf{x}^A) \cdot \mathbf{n}^A \quad (5.8.3)$$

$$f^C = -k_N g_N \quad \text{if } g_N < 0 \quad (5.8.4)$$

$k_n$  : Penalty coefficient

$\mathbf{x}^A, \mathbf{x}^B$  : Position vectors of point (A) on master segment and slave node (B)

$\mathbf{n}^A$  : Normal vector of point (A) on master segment

The penalty coefficient  $k_N$  has the effect of applying an elastic stiffness between the master segment and slave node, and the non-penetrated condition is satisfied approximately depending on the size. For the welded condition or the sliding contact condition, the contact force is assigned even when  $g_N$  is positive and the initially adjacent segment and slave nodes are not separated and its effects reflected. GTS NX automatically calculates the penalty coefficient using the following equation (5.8.5):

$$\begin{aligned} \text{plane/shell elements : } k_i &= \frac{f_s M_i}{h} A_{si} \\ \text{solid elements : } k_i &= \frac{f_s K_i}{h} A_{si} \end{aligned} \quad (5.8.5)$$

$f_s$  : Proportionality coefficient

$K_i$  : Bulk modulus

$M_i$  : Coefficient of expansion

$A_i$  : Area

$V_i$  : Volume

$h$  : Length of master segment solid :  $\frac{1}{n} \sum_i^n \frac{V_{mi}}{A_{mi}}$  plane/shell :  $\frac{1}{n} \sum_i^n A_{mi}^{1/2}$

The proportionality coefficient  $f_s$  above is determined differently depending on the analysis type or contact condition type, and the user can modify it to effectively satisfy the non-penetrated condition or welded condition. For the welded condition, a resistant force against sliding in the lateral direction of the contact plane is assigned and its size is as follows:

$$\mathbf{g}_T = \begin{Bmatrix} (\mathbf{u}^B - \mathbf{u}^A) \cdot \mathbf{t}_x^A \\ (\mathbf{u}^B - \mathbf{u}^A) \cdot \mathbf{t}_y^A \end{Bmatrix} \quad (5.8.6)$$

$$\mathbf{f}^T = k_T \mathbf{g}_T \quad (5.8.7)$$

$k_T$  : Penalty coefficient

$\mathbf{t}_x^A, \mathbf{t}_y^A$  : Lateral vector of point (A) on master segment

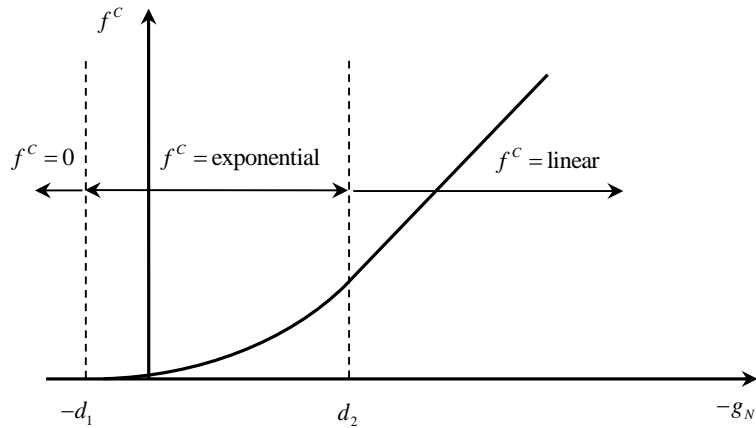
For the welded condition, the penalty coefficient  $k_T$  uses the same value as  $k_N$ .

As equation (5.8.4.) and (5.8.7), the contact force of linear elasticity or resistance force for sliding is not suitable for the general contact used in nonlinear analysis. In order to obtain the convergence, much oscillation can be occurred because the stiffness of general contact rapidly changes from 0 to

$k_N$  according to the sign of gap. To compensate for this, GTS NX uses the modified contact force as follows:

$$\begin{aligned}
 f^c &= 0 && \text{if } g_N > d_1 \\
 f^c &= \frac{f_0}{(\exp(1)-1)} \left[ \left( \frac{-g_N}{d_1} + 1 \right) \left( \exp\left( \frac{-g_N}{d_1} + 1 \right) - 1 \right) \right] && \text{if } -d_2 < g_N < d_1 \\
 f^c &= \frac{f_0}{(\exp(1)-1)} \left[ \left( \frac{d_2}{d_1} + 1 \right) \left( \exp\left( \frac{d_2}{d_1} + 1 \right) - 1 \right) \right] + k_N(-g_N - d_2) && \text{if } g_N < -d_2
 \end{aligned} \tag{5.8.8}$$

Figure 5.8.4 Relation between gap and modified contact force



There exists more complex nonlinearity in the resistance force against horizontal sliding because this force occurs only if the vertical force is applied. As a result, the equation (5.8.7) is modified and applied as follows:

$$\mathbf{f}^T = \frac{k_T f^c}{k_N d_2} \mathbf{g}_T \tag{5.8.9}$$

In the above equation, the discontinuity of force which may occur at the moment of contact suddenly disappeared can be minimized by proportion to the vertical contact force and horizontal force. In case of general contact, the friction can be considered additionally.

$$f = \|\mathbf{f}^T\| - \mu f^c \leq 0 \tag{5.8.10}$$

$\mu$  : Friction coefficient



---

The behavior which satisfied with the above equation becomes elastic movement, and if it does not satisfy the above equation due to the large horizontal movement, sliding occurs. When you compare (5.8.9) and (5.8.10), the horizontal relative displacement within certain distance  $d_2$  shows elastic movement, and the more relative displacement can be seen that the slip is assumed. As the general contact considering friction creates an asymmetric stiffness matrix, numerical calculated efficiency is significantly inhibited. Also, the large friction coefficient (over 0.3–0.4) or horizontal elastic modulus  $k_r$  can be the factors causing convergence problem.

## Section 9

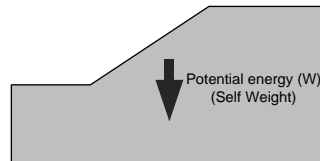
## Slope Stability Solution

Slope stability for an embankment or excavation is one of the most frequently dealt problems in geotechnical engineering. The slope always has a self-weight potential energy due to gravity and if external forces such as pore pressure, applied load, earthquake, wave force etc. act on the slope, its stability is greatly affected. Here, slope failure can occur when the active force of the slope is greater than the resistant force of the soil. Slope stability analysis evaluates the stability against failure using the relationship between the active force and resistant force of the slope.

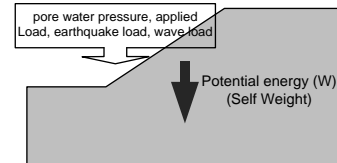
The widely used limit equilibrium method can only evaluate the stability for the basic given conditions. However, the actual collapse of the ground generates a large local deformation and fails at the limit. Hence, establishing an analysis method that can trace the deformed shape continuously from the initial deformation to collapse is important for stability analysis of the ground. Recently, active research is ongoing to apply finite element method as a method of evaluating stability such as slope failure, using the strengths of finite elements such as the ease in checking the deformed shape, even at various load and boundary conditions.

Figure 5.9.1 Slope failure process

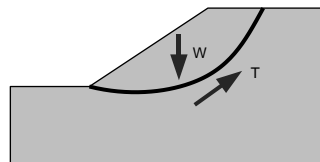
STEP #1 : Stable Ground Status



STEP #2 : Input the external Force



STEP #3 : Shear Stress within Slope



STEP #4 : Compute Factor of Safety

$$\text{Factor of Safety} = \frac{\text{Resisting force}}{\text{Driving Force}}$$



The following slope stability analysis methods have been suggested.

- ▶ Mass procedure and slice method according to the limit equilibrium theory
- ▶ Limit theory according to the rigid-plastic theory
- ▶ Finite element method according to the elasto-plastic theory

In GTS NX, the usable slope stability analysis methods that use the finite element method are the strength reduction method and the stress analysis method based on the limit equilibrium theory.

## 9.1 Strength Reduction Method

Slope stability analysis using the finite element method are detailed approximate solutions that satisfy all the equilibrium force conditions, compatibility conditions, constitutive equations and boundary conditions of each point on the slope. This numerical analysis method can simulate nearly actual failure shapes, reflect the field conditions better and can analyze the minimum safety factor and failure behavior of the slope in detail. Particularly, the failure process is automatically simulated without any assumptions made to the failure plane of the slope.<sup>9</sup>

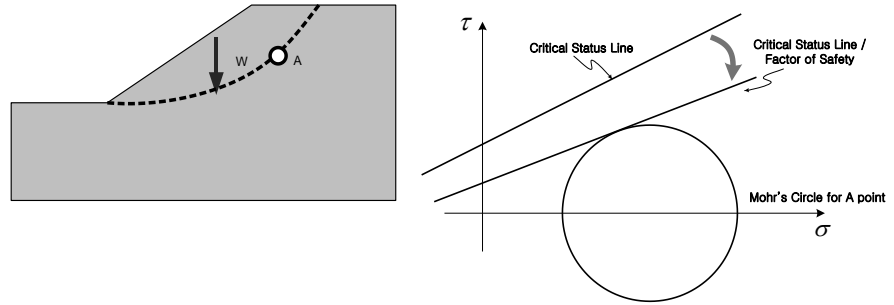
The strength reduction method (a slope stability analysis method based on the finite element method) gradually decreases the shear strength and performs analysis until the point where the calculation does not converge. This point is considered to be the failure point of the slope, and the maximum strength reduction ratio at this point is thought of as the minimum safety factor of the slope. This method is costly because it requires multiple nonlinear analyses, but it can provide more accurate results in a reasonable time for improved data processing speeds. Also, the strength reduction method can verify the deformation process from the initial slope to failure without any required assumptions for the failure plane.

### Strength reduction theory

To simulate slope failure using the strength reduction method, the safety factor is computed at an arbitrary point where the Mohr circle is in contact with the failure envelope, as shown in the figure below. The stress state at this point can be determined as the failure state and when this failure point increases, overall slope collapse occurs. The finite element analysis at this limit state diverges, and the safety factor at this point is defined as the minimum safety factor.

<sup>9</sup> Griffiths, D.V. and Lane, P.A. (1999). Slope Stability Analysis by Finite Elements, *Geotechnique*, 49(3), 387-403

Figure 5.9.2 Strength reduction method



#### Calculation of minimum safety factor

The material models used in the strength reduction method are Mohr Coulomb, Drucker Prager and Modified Mohr Coulomb. For the input variables used here, all variables are assumed to have a constant value except cohesion, friction angle and dilatency angle, which determine shear failure. The cohesion, friction angle and dilatency angle corresponding to ground elements (plane strain, axisymmetric, solid) are gradually decreased and the safety factor  $F_s$  at slope failure is computed.

$$F_s = \frac{\tau}{\tau_f} \quad (5.9.1)$$

Here,  $\tau$  is the shear strength of the slope material, and can be expressed using the Mohr-Coulomb criteria as follows:

$$\tau = c + \sigma_n \tan \phi \quad (5.9.2)$$

Also,  $\tau_f$  is the shear stress of the active plane and can be calculated as follows:

$$\tau_f = c_f + \sigma_n \tan \phi_f \quad (5.9.3)$$

$$c_f = \frac{c}{\text{SRF}} \quad \text{: Shear strength factor (Cohesion)}$$

$$\phi_f = \tan^{-1} \left( \frac{\tan \phi}{\text{SRF}} \right) \quad \text{: Shear strength factor (Friction angle)}$$

$$\text{SRF} \quad \text{: Strength reduction factor}$$

For the strength reduction method, the SRF value just before the non-convergence is evaluated as the safety factor. Hence, the safety factor can be slightly different depending on the user input number of convergence and convergence criteria.

Other material models can be included for slope safety analysis, but the strength reduction is not applied to these models.

#### Strength reduction using the arc-length method

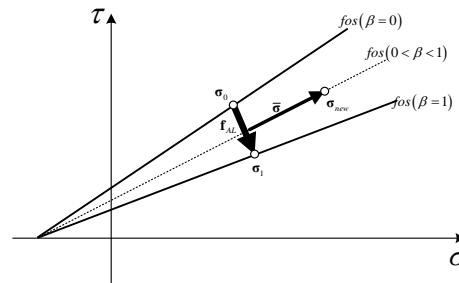
The main difference between the existing strength reduction method and the method using the arc-length method is the method of increasing/decreasing the safety factor, which is the standard for strength reduction. The existing method computes the safety factor of the next step by controlling the safety factor of the current step by the user defined increment. Hence, ineffective calculation is performed for very stable models or unstable models without the engineer's judgment because the uniform safety factor is incremented. However, using the arc-length method, the arc length is computed by the convergence speed of the previous step and thus a more appropriate safety factor increment can be obtained.

Defining the projected stress on the new failure plane caused by the strength decrease of the in-situ stress state  $\sigma_0$  as  $\sigma_1$ , and introducing an additional arc-length parameter  $\beta$  to apply the arc-length method, the stress within the element can be assumed as follows:

$$\sigma = (1 - \beta)\sigma_0 + \beta\sigma_1 + \bar{\sigma} \quad (5.9.4)$$

Here,  $\bar{\sigma}$  is the stress component corresponding to  $\beta$  that is needed to maintain the equilibrium with the external forces on the failure plane.

Figure 5.9.3 Arc-length load vector and stress flow diagram



Using equation (5.9.4), the unbalanced forces of the  $i$  th iterative calculation for nonlinear analysis can be expressed as a function of the DOF vector and arc-length parameter:

$$\mathbf{g}_i(\mathbf{u}_i, \beta_i) = \mathbf{f}_{ext} - \sum_e \int_{\Omega_e} \mathbf{B}^T [(1 - \beta)\sigma_0 + \beta\sigma_1 + \bar{\sigma}] d\Omega \quad (5.9.5)$$

The external force including self weight ( $\mathbf{f}_{ext}$ ) does not change with  $\beta$ . This method is different from the general arc-length method for unstable equilibrium state analysis in that the internal forces change with the stress assumption in equation (5.9.4). To apply the Newton-Raphson based nonlinear finite element analysis, equation (5.9.4) can be expanded for the incremental solution and increment parameters as shown below:

$$\mathbf{g}_{i+1} \cong \mathbf{g}_i - \mathbf{K}_{i+1} \delta \mathbf{u}_{i+1} + \delta \beta_{i+1} \mathbf{f}_{AL} = \mathbf{0} \quad (5.9.6)$$

$$\mathbf{K}_{i+1} = - \frac{\partial \mathbf{g}}{\partial \mathbf{u}} \quad : \text{Tangential stiffness matrix}$$

$$\mathbf{f}_{AL} = \frac{\partial \mathbf{g}}{\partial \beta} = \sum_e \int_{\Omega_e} \mathbf{B}^T \boldsymbol{\sigma}_0 d\Omega - \sum_e \int_{\Omega_e} \mathbf{B}^T \boldsymbol{\sigma}_1 d\Omega \quad : \text{Arc-length force vector}$$

Using this, the accumulated incremental solution that occurs at the  $i+1$ th iterative calculation is as follows:

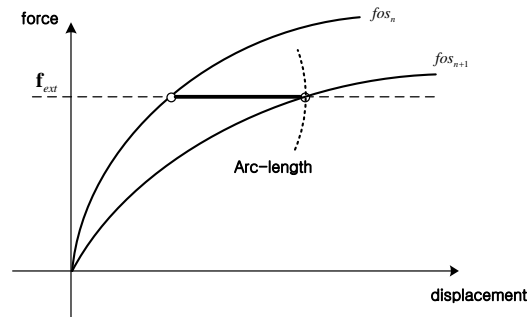
$$\Delta \mathbf{u}_{i+1} = \Delta \mathbf{u}_i + \delta \bar{\mathbf{u}} + \delta \beta_{i+1} \mathbf{u}_T \quad (5.9.7)$$

$$\delta \bar{\mathbf{u}} = \mathbf{K}_{i+1}^{-1} \mathbf{g}_i \quad : \text{Incremental solution for unbalanced force}$$

$$\mathbf{u}_T = \mathbf{K}_{i+1}^{-1} \mathbf{f}_{AL} \quad : \text{Displacement generated for arc-length load vector}$$

Here,  $\delta \beta_{i+1}$  is calculated using the arc-length constraint condition. The related information is already explained in the nonlinear solution section and is hence omitted. This process is repeated until the user defined convergence criteria is satisfied. The safety factor of each step can be calculated through this process. This subsequent process is also repeated until the rate of change for the safety factor is within a certain condition.

Figure 5.9.4 Safety factor increment for arc-length



## 9.2

### Stress Analysis Method

The limit equilibrium method is one of the most often used slope stability methods for actual design. However, this method cannot find the stress history of the actual slope or the change in ground behavior. On the other hand, slope stability analysis using the finite element method can consider the slope formation process and other ground characteristics, but it requires a longer analysis time because it performs multiple nonlinear analyses.

Recently, much research has been done in this area as to the strengths of the using limit equilibrium method and finite element based slope stability analysis simultaneously. GTS NX provides the slope stability analysis method that uses the finite element stress analysis results. This method is based on the virtual sliding surface of the limit equilibrium method and the stress results of stress analysis.

This method computes the safety factor for multiple assumed virtual sliding surfaces using the stress results of finite element analysis, and the minimum safety factor and corresponding critical section is computed. The provided ground material models are Mohr Coulomb, Drucker Prager and Modified Mohr Coulomb, just like the strength reduction method.

#### Calculation of minimum safety factor

The safety factor used in the finite element method is defined as follows:

$$F_s = \frac{\int_S \tau_f d\Gamma}{\int_S \tau_m d\Gamma} \quad (5.9.8)$$

Here,  $\tau_m$  is the generated shear stress,  $\tau_f$  the shear strength, and for Mohr Coulomb materials, it can be expressed as follows:

$$\begin{aligned} \tau_f &= c + \sigma_n \tan \phi \\ \tau_m &= \frac{1}{2}(\sigma_y - \sigma_x) \sin 2\theta + \tau_{xy} \cos 2\theta \end{aligned} \quad (5.9.9)$$

Here, the directional stress normal to the sliding surface  $\sigma_n$  is as follows:

$$\sigma_n = \sigma_x \sin^2 \theta + \sigma_y \cos^2 \theta - \tau_{xy} \sin 2\theta \quad (5.9.10)$$

$c$  : Cohesion

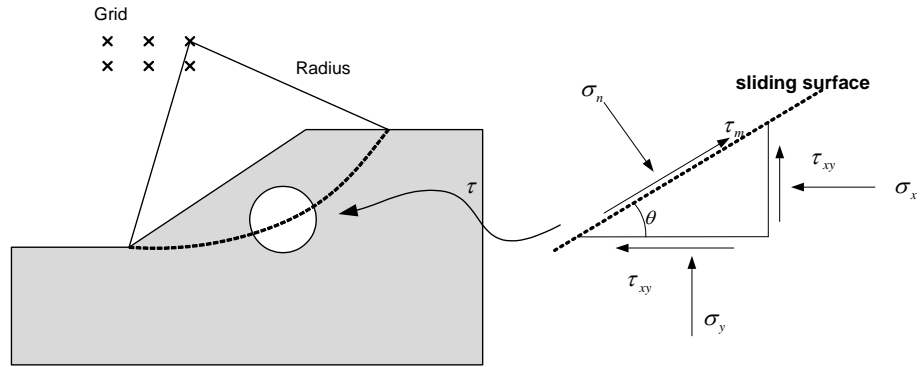
$\phi$  : Internal friction angle of the material

$\theta$  : Angle between horizontal plane and sliding surface

$\sigma_x, \sigma_y$  : Normal stress in the  $x$  direction and  $y$  direction respectively

$\tau_{xy}$  : Shear stress

Figure 5.9.5 Stress components of the slope



**Stress integration along virtual sliding plane**

To calculate the safety factor, the line integral of stresses along the virtual sliding plane need to be performed. For this, the stress value at an arbitrary position is required. The stress is calculated using the inner product of the nodal stress and the shape function at that position.

$$\sigma = \sum_{i=1}^{node} N_i \sigma_i^{node} \tag{5.9.11}$$

- $N_i$  : Shape function at node  $i$
- $\sigma_i^{node}$  : Nodal stress at node  $i$
- $\sigma$  : Stress at arbitrary point within the element

Here, the nodal stress is calculated through the stress recovery technique, which uses the nodal average method. In other words, GTS NX calculates the nodal stress through extrapolation of the integral stresses of each node sharing element, and the final nodal stress for shared nodes is applied as the average value of the calculated nodal stresses.

The stress integral along the virtual sliding plane in the 2D GCS is transformed into an integral form in 1D local coordinate system and calculated using the following equation:

$$\int_{n1}^{n2} \tau(x, y) d\Gamma = \frac{L}{2} \mathbf{T} \int_{-1}^1 \tau(\xi) d\xi = \frac{L}{2} \mathbf{T} \sum_{i=1}^{n_{int}} W_i \tau(\xi_i) \tag{5.9.12}$$

- $\xi$  : Coordinate variable in local coordinate system
- $W_i$  : Constant of integration at integral point  $i$
- $\mathbf{T}$  : Transformation matrix that transforms stress in the element coordinate system to GCS
- $L$  : Element length



$\tau$  : Shear stress  $\tau_m$  or shear strength  $\tau_f$  on virtual sliding plane

The finalized total safety factor for the given virtual sliding plane is as follows:

$$F_s = \frac{\sum_{i=1}^{nel} \int_{n_1}^{n_2} \tau_f d\Gamma}{\sum_{i=1}^{nel} \int_{n_1}^{n_2} \tau_m d\Gamma} \quad (5.9.13)$$

nel : Number of elements passing the virtual sliding plane

$n_1$  : Start point of the virtual sliding plane within the element

$n_2$  : End point of the virtual sliding plane within the element

The stress analysis method based on the limit equilibrium method uses the stress field computed from the finite element method and the virtual sliding surface of the limit equilibrium method. Hence, it has a stress distribution and deformed shape from finite element analysis, and is optimized for obtaining the critical section from the limit equilibrium method. Compared to the strength reduction method, it requires a much shorter analysis time and can accurately compute various ground or reinforcement members without any particular assumptions.

## Section 10

## Equivalent Linear Solution

Equivalent linear analysis simulates nonlinearly behaving ground according to strain using linear analysis. This method simplifies the complex nonlinear ground properties into linear equivalent properties for linear analysis. GTS NX supports free field analysis for analyzing the in-situ ground behavior before construction. GTS NX also supports 2D equivalent linear analysis for ground-structure coupled analysis.

## 10.1

## Free Field Analysis

## Method

Free field analysis finds the ground response for an input load on the in-situ ground state before any construction of structures. Free field analysis is used for ground surface vibration prediction to determine the design response spectrum, computation of dynamic stress and strain to evaluate liquefaction, and determination of earthquake load that causes ground or structural instability.

Free field analysis finds the ground response due to the vertically transmitted shear waves that pass the linear viscoelastic region. The analysis ground consists of multiple strata that are infinite in the horizontal direction and a semi-infinite bottom layer as shown in figure 5.10.1. Each stratum is homogeneous and assumed to have isotropic material properties. The vibrations in the analysis model are caused by shear waves, which penetrate and reflect the model ground vertically, and displacement only occurs in the horizontal direction. Hence, the wave equation (5.10.1) needs to be satisfied for all strata.

$$\rho \frac{\partial^2 u}{\partial t^2} = G \frac{\partial^2 u}{\partial x^2} + 2\xi G \frac{\partial^3 u}{\partial x^2 \partial t} \quad (5.10.1)$$

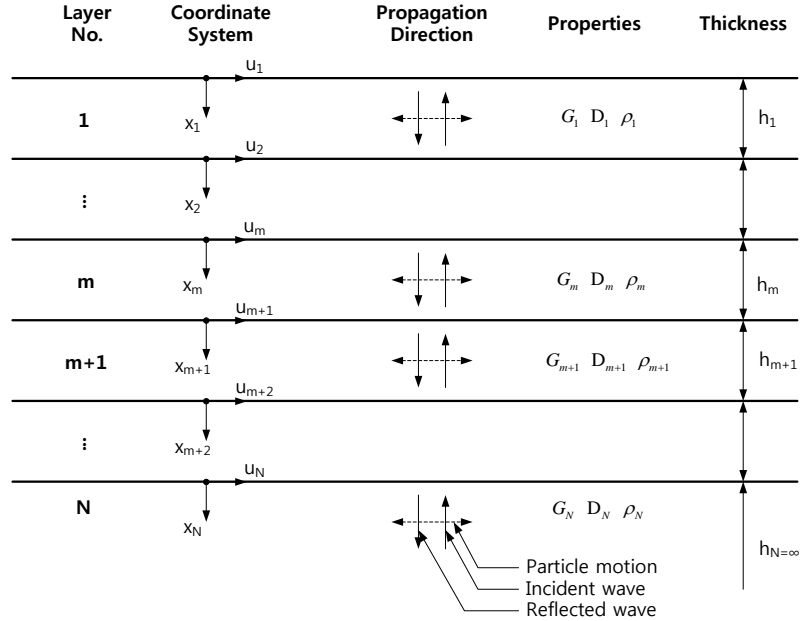
$u$  : Horizontal displacement

$\rho$  : Mass density

$G$  : Shear modulus

$\xi$  : Hysteretic damping ratio

Figure 5.10.1 Free field analysis model



Representing the displacement function as a harmonic function like equation (5.10.2) and transforming equation (5.10.1) into the frequency domain gives the governing equation (5.10.3), and the stress-displacement relationship is equation (5.10.4).

$$u(x, t) = u(x, \omega)e^{i\omega t} \quad (5.10.2)$$

$$G^* \frac{\partial^2}{\partial x^2} u(x, \omega) - \rho\omega^2 u(x, \omega) = 0 \quad (5.10.3)$$

$$\tau(x, \omega) = G^* \frac{\partial}{\partial x} u(x, \omega) \quad (5.10.4)$$

$\tau(x, \omega)$  : Shear stress in frequency domain

$G^*$  : Complex shear modulus

The complex shear modulus above<sup>10</sup> uses the following equation suggested by Udaka.

$$G^* = G(1 - 2\xi^2 + i2\xi\sqrt{1 - \xi^2}) \quad (5.10.5)$$

<sup>10</sup> Udaka, Takekazu. (1975). Analysis of Response of Large Embankments to Traveling Base Motions, Department of Civil and Environmental Engineering. Berkeley: University of California, p346.

The free field ground model is generally expressed as figure 5.10.1 to find the solution of the 1D wave transmission equation. The layer boundary number is assigned from the ground surface and expressing the response of the  $m$  th layer as  $u_m$ , the response can be represented using the following function of the depth  $x_m$  from the top part of the  $m$  th layer:

$$u_m(x_m, \omega) = A_m(\omega)e^{ik_m^*x_m} + B_m(\omega)e^{-ik_m^*x_m} \quad (5.10.6)$$

$$\tau_m(x_m, \omega) = ik_m^*G_m^*(A_m(\omega)e^{ik_m^*x_m} - B_m(\omega)e^{-ik_m^*x_m}) \quad (5.10.7)$$

$k_m^*$  : Wave number of the  $m$  th layer

$A_m$  : Layer response coefficient of elastic waves transferred upwards in the  $m$  th layer

$B_m$  : Layer response coefficient of elastic waves transferred downwards in the  $m$  th layer

The following compatibility condition and force equilibrium condition need to be satisfied at the adjacent layer boundaries:

$$\begin{cases} u_m(x_m = h_m) = u_{m+1}(x_{m+1} = 0) \\ \tau_m(x_m = h_m) = \tau_{m+1}(x_{m+1} = 0) \end{cases} \quad m = 1, 2, \dots, (N-1) \quad (5.10.8)$$

Substituting equations (5.10.6) and (5.10.7) into equation (5.10.8) can derive the relationship between the coefficients as follows:

$$\begin{cases} A_{m+1} + B_{m+1} = A_m e^{ik_m^*h_m} + B_m e^{-ik_m^*h_m} \\ A_{m+1} - B_{m+1} = \frac{k_m^* G_m^*}{k_{m+1}^* G_{m+1}^*} (A_m e^{ik_m^*h_m} - B_m e^{-ik_m^*h_m}) \end{cases}, \quad m = 1, 2, \dots, (N-1) \quad (5.10.9)$$

Rearranging this to derive the relationship between the response coefficients of adjacent ground layers gives the following recurrence relationship shown in equation (5.10.10):

$$\begin{aligned} A_{m+1} &= \frac{1}{2} A_m (1 + \alpha_m^*) e^{ik_m^*h_m} + \frac{1}{2} B_m (1 - \alpha_m^*) e^{-ik_m^*h_m} \\ B_{m+1} &= \frac{1}{2} A_m (1 - \alpha_m^*) e^{ik_m^*h_m} + \frac{1}{2} B_m (1 + \alpha_m^*) e^{-ik_m^*h_m} \end{aligned} \quad (5.10.10)$$

$h_m$  : Thickness of  $m$  th layer

$\alpha_m^*$  : Dynamic stiffness ratio between adjacent layers

Here, the dynamic stiffness ratio between adjacent layers can be expressed as follows:

$$\alpha_m^* = \frac{k_m^* G_m^*}{k_{m+1}^* G_{m+1}^*} \quad (5.10.11)$$

Because shear stress is always '0' at the ground surface,  $A_1 = B_1$  can be known from equation (5.10.7). Hence, the response coefficient of the  $m$  th layer can be found by applying equation (5.10.10) in order from the first layer.

$$\begin{aligned} A_m(\omega) &= a_m(\omega)A_1(\omega) \\ B_m(\omega) &= b_m(\omega)B_1(\omega) \end{aligned} \quad (5.10.12)$$

Here,  $a_1 = b_1 = 1$  can be known. The transfer function  $\mathbf{H}_{ij}(\omega)$  between layer boundary  $i$  and layer boundary  $j$  is as follows:

$$H_{ij}(\omega) = \frac{u_i(\omega)}{u_j(\omega)} = \frac{a_i(\omega) + b_i(\omega)}{a_j(\omega) + b_j(\omega)} \quad (5.10.13)$$

If the transfer function  $H_{ij}(\omega)$  is determined and the response  $u_j(\omega)$  at layer boundary  $j$  is given, the response  $u_i(\omega)$  at layer boundary  $i$  can be found using the following equation:

$$u_i(\omega) = H_{ij}(\omega)u_j(\omega) \quad (5.10.14)$$

Also, frequency domain response can be inverted to the time domain using the FFT (fast Fourier transform) method.

## 10.2

### 2D Equivalent Linear Analysis

The main difference between ground-structure interaction problems and general structural dynamics problems is the radiation damping phenomena due to the infinite ground domain. Whilst general damping properties damp the structural motion through material friction, radiation damping releases wave energy into the infinite domain of the ground, which contributes to the damping phenomena of structural kinetic energy.

Radiation damping is included in the damping term of the equation of motion, and its size is determined by the wave form of the externally transmitted wave. The wave form can be easily modeled in the frequency domain and it is efficient to consider this using frequency domain solvers. General ground materials are fundamentally heterogeneous and the nonlinearity of its mechanical behavior is very severe.

To correctly analyze the ground-structure interaction problem, the radiation damping phenomena above and important nonlinearity characteristics need to be considered simultaneously. Hence, the

frequency domain solver is used for easy modeling of radiation damping and the equivalent linear method is used to analyze material nonlinearity.

The analysis process uses the frequency domain analysis process that uses FFT (fast Fourier transform) and the equation of motion composes a combined ground-structural system that has the free field response as the input motion. Hence, the ground response and structural response are obtained together for one computation. Interpolation is used to reduce the number of frequencies where the solution to the equation of motion needs to be found, and this method uses the interpolation of the transfer function solutions of two continuous frequencies. Hence, the setting of basic frequencies is important and a sufficiently high limit frequency needs to be defined to secure validity of the ground motion analysis.

As mentioned above, the input motion in the time domain can be converted to the frequency domain using FFT to calculate the structural response under a vibration load with a constant frequency. All loads in frequency response analysis are defined in the frequency domain and are expressed as functions of the assigned frequency. In other words, when the angular excitation frequency is  $\omega$ , the load in frequency response analysis can be expressed as the following complex harmonic function:

$$\mathbf{f}(t) = \mathbf{f}(\omega)e^{i\omega t} \quad (5.10.15)$$

The corresponding response can also be expressed in the same form:

$$\mathbf{u}(t) = \mathbf{u}(\omega)e^{i\omega t} \quad (5.10.16)$$

Using this, the equation of motion can be expressed in the following form:

$$[-\omega^2 \mathbf{M} + i\omega \mathbf{C} + \mathbf{K}] \mathbf{u}(\omega) = \mathbf{f}(\omega) \quad (5.10.17)$$

Using equation (5.10.5) suggested by Udaka, the equation above can be modified and rearranges into the following equation:

$$[-\omega^2 \mathbf{M} + \mathbf{K}^*] \mathbf{u}(\omega) = \mathbf{f}(\omega) \quad (5.10.18)$$

$\mathbf{K}^* = \mathbf{K}(1 - 2\xi^2 + i2\xi\sqrt{1 - \xi^2})$  : Complex stiffness coefficient

#### Energy transmitting boundary

It is difficult to model the nearly infinite ground accurately using the 2D model used for ground-structure analysis. Hence, the model boundary needs to be set at an engineering appropriate position and the set boundaries need to be processed to simulate actual site conditions.

GTS NX uses the energy transmitting boundary suggested by Lysmer and Wass<sup>11</sup> to express the load  $\mathbf{f}(\omega)$  in equation (5.10.18) as follows:

$$\mathbf{f}(\omega) = \mathbf{K}_f^* \mathbf{u}_f(\omega) + (\mathbf{R} + \mathbf{L})(\mathbf{u}(\omega) - \mathbf{u}_f(\omega)) \quad (5.10.19)$$

$\mathbf{u}_f(\omega)$  : Free field analysis displacement of the transmit boundary

$\mathbf{K}_f^*$  : Complex stiffness matrix of the transmit boundary

$\mathbf{R}$  : Stiffness matrix of the right transmit boundary

$\mathbf{L}$  : Stiffness matrix of the left transmit boundary

#### Direct frequency response analysis

When using the direct solver for direct frequency response analysis, solving the simultaneous equation (5.10.18) gives the frequency response  $\mathbf{u}(\omega)$ . The solution can be found accurately using the direct method, but calculation is very inefficient for large problems or when many frequencies exist because the simultaneous equation needs to be recomposed and solved for each frequency. To supplement this, efficient analysis can be performed by interpolation using the transfer function.

#### Enforced motion

The input motion of equivalent linear analysis is generally earthquake loading. GTS NX performs analysis that use enforced motion. First, the equilibrium equation (5.10.17) is separated into DOFs with and without enforced motion.

$$\begin{bmatrix} \mathbf{M}_{11} & \mathbf{M}_{12} \\ \mathbf{M}_{21} & \mathbf{M}_{22} \end{bmatrix} \begin{Bmatrix} \ddot{\mathbf{u}}_1 \\ \ddot{\mathbf{u}}_2 \end{Bmatrix} + \begin{bmatrix} \mathbf{C}_{11} & \mathbf{C}_{12} \\ \mathbf{C}_{21} & \mathbf{C}_{22} \end{bmatrix} \begin{Bmatrix} \dot{\mathbf{u}}_1 \\ \dot{\mathbf{u}}_2 \end{Bmatrix} + \begin{bmatrix} \mathbf{K}_{11} & \mathbf{K}_{12} \\ \mathbf{K}_{21} & \mathbf{K}_{22} \end{bmatrix} \begin{Bmatrix} \mathbf{u}_1 \\ \mathbf{u}_2 \end{Bmatrix} = \begin{Bmatrix} \mathbf{f}_1 \\ \mathbf{f}_2 \end{Bmatrix} \quad (5.10.20)$$

$\mathbf{u}_1$  : Displacement of unconfined DOF

$\mathbf{u}_2$  : Displacement of DOF confined by enforced motion

$\mathbf{f}_1$  : Load acting on unconfined DOF

$\mathbf{f}_2$  : Confining force of DOF confined by enforced motion

Separating the unconfined DOF displacement  $\mathbf{u}_1$  into the following quasi-static displacement  $\mathbf{u}_1^{qs}$  and dynamic relative displacement  $\mathbf{y}$  is as follows:

<sup>11</sup> Lysmer, J. and Wass, G. (1972). Shear waves in plane infinite structures. Proc. ASCE, Vol. 98, EM1, pp. 85-105.

$$\begin{aligned}
 \mathbf{u}_1 &= \mathbf{u}_1^{qs} + \mathbf{y} \\
 \dot{\mathbf{u}}_1 &= \dot{\mathbf{u}}_1^{qs} + \dot{\mathbf{y}} \\
 \ddot{\mathbf{u}}_1 &= \ddot{\mathbf{u}}_1^{qs} + \ddot{\mathbf{y}}
 \end{aligned}
 \tag{5.10.21}$$

The quasi-static displacement, velocity, and acceleration can be calculated using the following equations:

$$\begin{aligned}
 \mathbf{u}_1^{qs} &= -\mathbf{K}_{11}^{-1} \mathbf{K}_{12} \mathbf{u}_2 \\
 \dot{\mathbf{u}}_1^{qs} &= -\mathbf{K}_{11}^{-1} \mathbf{K}_{12} \dot{\mathbf{u}}_2 \\
 \ddot{\mathbf{u}}_1^{qs} &= -\mathbf{K}_{11}^{-1} \mathbf{K}_{12} \ddot{\mathbf{u}}_2
 \end{aligned}
 \tag{5.10.22}$$

Dynamic relative displacement, relative velocity, and relative acceleration are expressed as follows:

$$\begin{aligned}
 \mathbf{y} &= \mathbf{u}_1 - \mathbf{u}_1^{qs} \\
 \dot{\mathbf{y}} &= \dot{\mathbf{u}}_1 - \dot{\mathbf{u}}_1^{qs} \\
 \ddot{\mathbf{y}} &= \ddot{\mathbf{u}}_1 - \ddot{\mathbf{u}}_1^{qs}
 \end{aligned}
 \tag{5.10.23}$$

Also, frequency domain analysis results can be found by inverting to the time domain using the FFT (fast Fourier transform) method.

